

**THE ENDOPLASMIC RETICULUM UDPASE ENTPD5 PROMOTES
CANCER CELL GROWTH AND SURVIVAL IN THE PI3K/PTEN
PATHWAY**

APPROVED BY SUPERVISORY COMMITTEE

Xiaodong Wang, Ph.D

George DeMartino, Ph.D

Jose Rizo-Rey, Ph.D

Hongtao Yu, Ph.D

Melanie Cobb, Ph.D

ACKNOWLEDGEMENTS

I would like to express my gratitude to several people that have supported me over the last five years. I would not be able to finish my thesis work if it were not for all of their support.

I would like to thank my mentor, Dr. Xiaodong Wang. He is the best mentor you could ever wish for. He offered patience and his full support as he taught me how things should be done. As he said, we should “aim high, start low”, “read more”, “start preliminary test when you have ideas” and “ask for help when you need it”. This is the essence how science is done in Wang Lab. He has been very patient with all his students and he cares about them. He trains students to raise questions, develop hypothesis, and execute experiments, independently. While Xiaodong encouraged us to work independently, he is always there for us whenever he is needed. His wisdom and expertise helped me grow from a bioinformatics student to a biochemist who can work independently. I feel privileged to learn from him.

I am also as grateful to the members of my thesis committee Drs. George DeMartino, Jose Rizo-Rey, Hongtao Yu and Melanie Cobb. I greatly appreciate their encouragement throughout my graduate study. They shared their enthusiasm toward science with me and inspired me to pursue the important scientific questions.

I am in debt to Drs. Yi Liu, Qinghua Liu, Benjamin Tu, Jake Chen and Jer-Tsong Hsieh and Ms. Leeju Wu for all their help, support and encouragements that paved the way for my matriculation to UT Southwestern.

I would like to also thank to the ENTPD5 team: Drs. Min Fang, Liping Zhao and Mr. Song Huang for collaboration, discussion and help.

I am also thankful to Wang Lab family, Drs. Zhigao Wang, Fenghe Du, Lai Wang, Gelin Wang, Wenhua Gao, Hui Jiang, Sudan He, Huayi Wang, also my colleagues Libin Shang, Greg Kunkel, Liming Sun, Hong Yu, Xian Jiang for their friendship, help and support.

And last, I want to thank my family for their strong support for my whole life.

**THE ENDOPLASMIC RETICULUM UDPASE ENTPD5 PROMOTES
CANCER CELL GROWTH AND SURVIVAL IN THE PI3K/PTEN
PATHWAY**

By

Zhirong Shen

DISSERTATION

Presented to the Faculty of the Graduate School of Biomedical Sciences

The University of Texas Southwestern Medical Center at Dallas

In Partial Fulfillment of the Requirements

For the Degree of

DOCTOR OF PHILOSOPHY

The University of Texas Southwestern Medical Center at Dallas

Dallas, Texas

Oct, 2010

Copyright

by

Zhirong Shen, 2010

All Rights Reserved

**THE ENDOPLASMIC RETICULUM UDPASE ENTPD5 PROMOTES
CANCER CELL GROWTH AND SURVIVAL IN THE PI3K/PTEN
PATHWAY**

Zhirong Shen, M.S.

The University of Texas Southwestern Medical Center at Dallas, 2010

Supervising Professor: Xiaodong Wang, Ph.D.

PI3 Kinase and PTEN lipid phosphatase control the level of cellular phosphatidylinositol (3,4,5)-trisphosphate, an activator of AKT kinase that promotes cell growth and survival. Mutations activating AKT are commonly observed in human cancers. Activation of AKT and downstream PI3 Kinase signaling promotes protein translation, resulting in increased protein flux into ER; this will lead to decreased efficiency of protein folding and accumulation of unfolded proteins in the ER and finally lead to ER stress. How does cancer cell solve this problem of increased folding during

rapid growth to avoid ER stress? We discovered that ENTPD5, an endoplasmic reticulum (ER) enzyme, is up-regulated in cell lines and primary human tumor samples with active AKT. AKT upregulates ENTPD5 by relieving transcriptional inhibition by FoxO transcription factors. ENTPD5 hydrolyzes UDP to UMP to promote protein N-glycosylation and folding in ER. Knockdown of ENTPD5 in PTEN-null cells causes ER stress and loss of receptor tyrosine kinases through ER-associated degradation pathway under stress conditions. Consequently, the growth of PTEN-null cells is inhibited both in vitro and in mouse xenograft tumor models. ENTPD5 is therefore an essential component for PI3K/AKT active cancer cells and a potential drug target for anti-cancer therapy.

TABLE OF CONTENTS

PRIOR PUBLICATIONS.....	x
LIST OF FIGURES.....	xi
LIST OF ABBREVIATIONS.....	xii
CHAPTER ONE: <i>Introduction</i>	1
Receptor Tyrosine Kinase (RTK) signaling pathway	1
Quality control of glycosylated proteins in Endoplasmic Reticulum	3
RTK, PI3K and Glycosylation.....	4
Figures.....	6
References.....	9
Chapter two: <i>Purification and characterization of ENTPD5</i>	10
Introduction.....	10
PETN knockout MEFs have an elevated activity that hydrolyze ATP to AMP.....	11
ENTPD5 is responsible for the elevated ATPase activity in PTEN knockout cells...	13
UMP or GMP is a required co-factor for the ATP hydrolysis activity.....	15
ENTPD5, UMP kinase, and Adenylate kinase constitute an ATP to AMP hydrolysis Cycle.....	16
Materials and Methods.....	20
Figures.....	28
References.....	42
CHAPTER THREE: <i>Regulation of Entpd5 by PI3K/AKT signaling pathway</i>	43

Introduction.....	43
Regulation of Entpd5 by PI3K/AKT signaling pathway through FoxO family transcription factor.....	44
Microarray data analysis revealed correlation of expression of Entpd5 with activation of RTK/PI3K signaling pathway.....	45
ENTPD5 expression correlates with AKT activation in human cancer cell lines and primary tumor samples.....	47
Materials and Methods.....	49
Figures.....	51
References.....	61
CHAPTER FOUR: <i>in vivo</i> function of Entpd5	64
Introduction.....	64
Knockdown of Entpd5 causes cell death under protein-overload conditions.....	66
Knockdown of Entpd5 causes ER stress under protein-overload conditions.....	67
EGFR are degraded in ER-associated degradation pathway.....	68
Knockdown of Entpd5 causes tumor shrinkage in xenograft model.....	69
Materials and Methods.....	72
Figures.....	76
References.....	89
SUMMARY	92
VITAE	95

Prior publications

1. Xue W, Wang J, **Shen Z**, Zhu H. (2004). Enrichment of transcriptional regulatory sites in non-coding genomic region. *Bioinformatics* 20(4): 569-75
2. Fang M, **Shen Z**, Huang S, Zhao L, Chen S, Mak, T. and Wang X. (2010). The Endoplasmic Reticulum UDPase ENTPD5 Promotes Cell Growth and Survival in the PI3K/PTEN Pathway. *Cell*. 2010 Nov 24;143(5):711-24.

LIST OF FIGURES

CHAPTER ONE

Figure 1-16

CHAPTER TWO

Figure 2-1.....28

Figure 2-2.....31

Figure 2-3.....35

Figure 2-4.....38

Figure 2-5.....41

CHAPTER THREE

Figure 3-1.....51

Figure 3-2.....53

Figure 3-3.....56

Figure 3-4.....58

Figure 3-5.....60

CHAPTER FOUR

Figure 4-1.....76

Figure 4-2.....78

Figure 4-3.....80

Figure 4-4.....82

Figure 4-5.....84

Figure 4-6.....85

Figure 4-7.....88

LIST OF ABBREVIATIONS

AK1: Adenylate Kinase 1

CMPK: Cytidine/Uridine Monophosphate Kinase

CNX/CRT: Calnexin/calreticulin

EGFR: Epidermal growth factor receptor

HER2: Human EGFR-Related 2

PIP2: Phosphatidylinositol 4,5-bisphosphate

PIP3: Phosphatidylinositol 3,4,5-trisphosphate

PTEN: Phosphatase and tensin homolog deleted from chromosome ten

RTK: Receptor Tyrosine Kinase

TFBS: Transcription factor binding sites

TSC2: Tuberous sclerosis 2

UGGT: UDP-Glucose:Glycoprotein glucotransferase

Chapter 1: Introduction

Receptor Tyrosine Kinase (RTK) signaling pathway

Receptor Tyrosine Kinases (RTKs) are a group of high affinity receptors for cytokines and growth factors. Activation of RTKs has been shown to have critical role in the progression of many types of cancer. Activation of RTKs by their ligand such as growth factors usually leads to autophosphorylation of key tyrosine residues in the activation loops, resulting in stimulation of receptor's tyrosine kinase activity (Gschwind et al., 2004).

PI3K/AKT and MAPK/ERK signaling pathways have been shown to be activated by RTKs, relaying the kinase cascades and mediating cellular responses such as cell proliferation and anti-apoptosis. PI3K phosphorylates phosphatidylinositol 4,5-bisphosphate (PIP₂) at the 3-OH position of the inositol ring to generate phosphatidylinositol 3,4,5-trisphosphate (PIP₃), which recruits phosphatidylinositol-dependent kinase 1 (PDK1), and serine/threonine kinase AKT to plasma membrane by binding to their pleckstrin homology domains(Whitman et al., 1988). PDK1 further phosphorylates and activates AKT(Stephens et al., 1998; Stokoe et al., 1997). Subsequently, AKT phosphorylates many downstream cellular targets including TSC2 (tuberous sclerosis 2) protein, resulting in activation of the rapamycin-sensitive mTORC1 complex(Gao et al., 2002; Inoki et al., 2002). mTORC1 complex phosphorylates p70S6K1(p70 S6 Kinase 1) and 4E-BP1(eukaryotic initiation factor 4E Binding Protein 1) to accelerate translational

rate to accommodate rapid growth (Brown et al., 1995; Burnett et al., 1998).

PTEN(**P**hosphatase and **t**ensin homolog deleted from chromosome **ten**) is a lipid phosphatase and it antagonizes the PI3K signaling by dephosphorylating PIP3 back to PIP2 (Maehama and Dixon, 1998).

The importance of RTK signaling has been manifested by numerous reports that many RTKs are highly activated in many types of human cancers. The most studied RTK, EGFR (epidermal growth factor receptor) has been reported to be over-expressed and highly activated. In addition, EGFR family members HER2(Human EGFR-Related 2) has also been shown to play a critical role in the pathogenesis of breast cancer and ovarian cancer(Gschwind et al., 2004).

PI3K also play a crucial role in tumor progression. In addition to be directly activated by RTKs and Ras oncogene, the gene encoding the catalytic subunit p110a, PI3KCA, frequently harbors activating mutations in high percentage of gastric, colon, breast and lung cancers(Samuels et al., 2004). The catalytic subunit of PI3Ka is also amplified in ovarian cancer and breast cancer(Campbell et al., 2004).

The PI3K antagonist PTEN is the second most commonly mutated tumor suppressor gene after p53. Mutations and deletions that inactivate its phosphatase activity frequently occur in glioblastoma, endometrial cancer, prostate cancer, and reduced expression of PTEN is found in many other tumor types such as lung and breast cancer, leading to increased cell proliferation and reduced cell death(Keniry and Parsons, 2008)

The importance of PTEN in cancer is further emphasized by mouse models of PTEN deletion. The homozygous loss of PTEN is embryonic lethal, however, heterozygous loss of PTEN leads to neoplastic change in prostate, thyroid, colon, lymphatic system, mammary gland and endometrium, demonstrating that haploinsufficiency of PTEN promotes cancer formation (Di Cristofano et al., 1998; Podsypanina et al., 1999). The embryonic fibroblasts from PTEN null mice (MEFs) exhibit resistance to many apoptotic stimuli such as UV irradiation, growth factor withdrawal, TNF α and heat shock compared to PTEN heterozygous MEF cells (Stambolic et al., 1998).

Quality control of glycosylated proteins in Endoplasmic Reticulum

After synthesis, proteins must fold correctly to perform biological functions. Many secreted proteins and membrane proteins are synthesized on ER-bound ribosomes and are co-translationally inserted into ER lumen where they are glycosylated at the asparagines (Asn) sites of Asn-X-Ser/Thr consensus sequence and obtain their native structure before being exported to Golgi apparatus or other compartments for further modification.

There is a well-characterized quality control system called calnexin/calreticulin reglucosylation cycle in the ER. CRT/CRX binds only to monoglucosylated glycan. Two enzymes control cycle of this quality control system by cleaving and adding glucose from misfolded glycoproteins. Glucosidase II cleaves glucose from high mannose and UGGT1 adds glucose to high mannose. The removal and addition of

glucose allows the binding and release of calnexin/calreticulin (CNX/CRT) until the target proteins are correctly folded and transported to next compartments such as Golgi apparatus or the proteins are targeted for degradation by ER associated degradation if the unfolded proteins are misfolded beyond repair (Hebert et al., 2009; Matsumoto et al., 2008; Molinari, 2007; Ruddock and Molinari, 2006).

RTK, PI3K and Glycosylation

RTKs such EGFR, HER2 and IGFR are highly glycosylated in cancer cells. N-glycosylation is well tuned and regulated in ER. N-glycosylation is very critical for RTK maturation and ligand-induced activation (Hakomori, 2002). Inhibition of N-glycosylation by tunicamycin has been shown to reduce IGFR and EGFR in malignant cancer cells (Dricu et al., 1997). Since activation of RTK signaling and downstream PI3K signaling promotes protein translation, resulting in increased protein flux into ER, this will lead to decreased efficiency of protein folding and accumulation of unfolded proteins in the ER and finally lead to ER stress. How does cancer cell solve this problem of increased folding during rapid growth to avoid ER stress?

In my dissertation I want to discuss the questions above. Serendipitously, we discovered that an ER-localized UDPase ENTPD5 is responsive to PI3K/AKT activation during our study of the reason for resistance to apoptosis of PTEN null MEF cells (led by Dr. Min Fang). This enzyme may promote protein reglucosylation,

thereby facilitating protein folding and maintaining RTK glycosylation. In Chapter 2, we purified ENTPD5 and other components from PTEN null MEF cells using extensive biochemical fractionation. I was involved in characterization of response of ENTPD5 to PTEN signaling. In Chapter 3, I will present how Entpd5 is regulated by PI3K/AKT signaling pathway. Finally, I want to discuss detailed mechanism of how ENTPD5 inhibits protein-overloading induced ER stress and apoptosis, and the importance of this enzyme for tumor growth and survival *in vivo*.

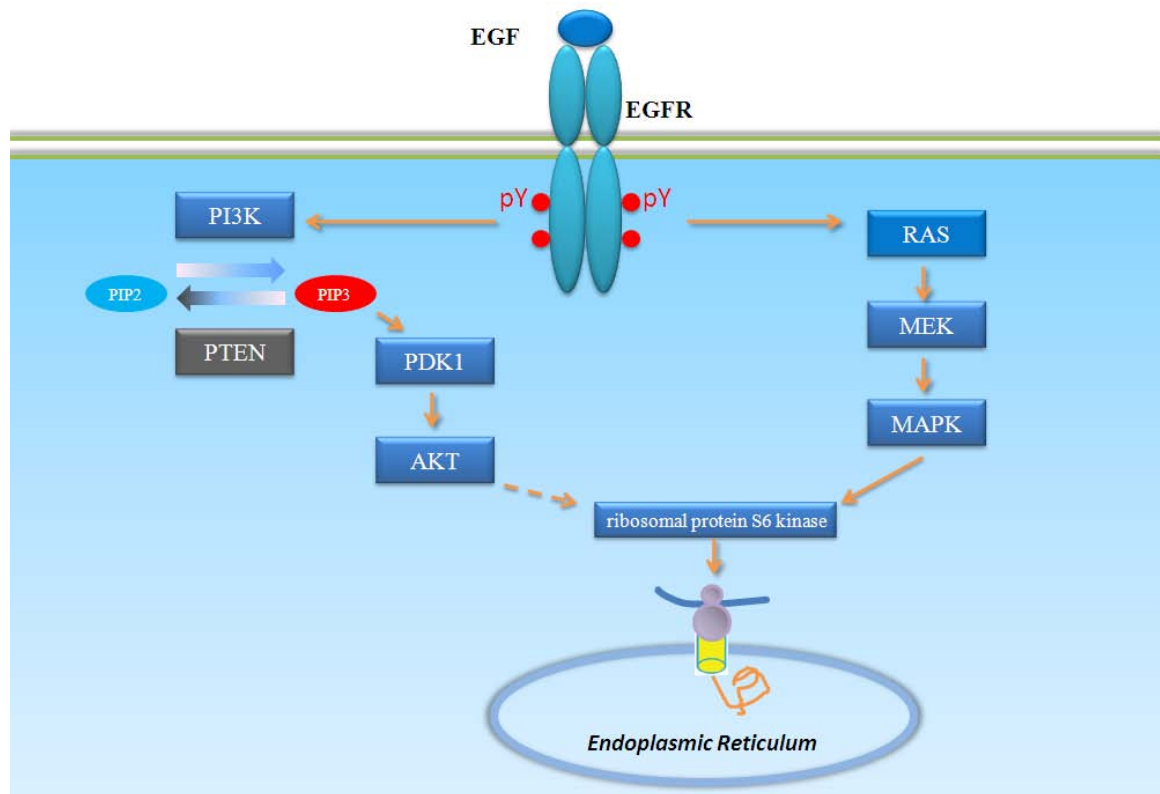


Figure 1-1 Receptor tyrosine kinase and PTEN signaling pathway.

Activation of Receptor tyrosine kinase and inactivation of PTEN in cancers will lead to upregulation of protein synthesis. Most of the proteins required protein glycosylation in Endoplasmic Reticulum. How does cancer cell deal with increased stress generated during protein folding remains an interesting question.

Reference

- Brown, E.J., Beal, P.A., Keith, C.T., Chen, J., Shin, T.B., and Schreiber, S.L. (1995). Control of p70 s6 kinase by kinase activity of FRAP in vivo. *Nature* 377, 441-446.
- Burnett, P.E., Barrow, R.K., Cohen, N.A., Snyder, S.H., and Sabatini, D.M. (1998). RAFT1 phosphorylation of the translational regulators p70 S6 kinase and 4E-BP1. *Proc Natl Acad Sci U S A* 95, 1432-1437.
- Campbell, I.G., Russell, S.E., Choong, D.Y.H., Montgomery, K.G., Ciavarella, M.L., Hooi, C.S.F., Cristiano, B.E., Pearson, R.B., and Phillips, W.A. (2004). Mutation of the PIK3CA Gene in Ovarian and Breast Cancer. *Cancer Research* 64, 7678-7681.
- Di Cristofano, A., Pesce, B., Cordon-Cardo, C., and Pandolfi, P.P. (1998). Pten is essential for embryonic development and tumour suppression. *Nat Genet* 19, 348-355.
- Dricu, A., Carlberg, M., Wang, M., and Larsson, O. (1997). Inhibition of N-linked Glycosylation Using Tunicamycin Causes Cell Death in Malignant Cells: Role of Down-Regulation of the Insulin-like Growth Factor 1 Receptor in Induction of Apoptosis. *Cancer Res* 57, 543-548.
- Gao, X., Zhang, Y., Arrazola, P., Hino, O., Kobayashi, T., Yeung, R.S., Ru, B., and Pan, D. (2002). Tsc tumour suppressor proteins antagonize amino-acid-TOR signalling. *Nat Cell Biol* 4, 699-704.
- Gschwind, A., Fischer, O.M., and Ullrich, A. (2004). The discovery of receptor tyrosine kinases: targets for cancer therapy. *Nat Rev Cancer* 4, 361-370.
- Hakomori, S. (2002). Glycosylation defining cancer malignancy: New wine in an old bottle. *Proceedings of the National Academy of Sciences of the United States of*

America 99, 10231-10233.

Hebert, D.N., Bernasconi, R., and Molinari, M. (2009). ERAD substrates: Which way out? *Seminars in Cell & Developmental Biology* 21, 526-532.

Inoki, K., Li, Y., Zhu, T., Wu, J., and Guan, K.-L. (2002). TSC2 is phosphorylated and inhibited by Akt and suppresses mTOR signalling. *Nat Cell Biol* 4, 648-657.

Keniry, M., and Parsons, R. (2008). The role of PTEN signaling perturbations in cancer and in targeted therapy. *Oncogene* 27, 5477-5485.

Maehama, T., and Dixon, J.E. (1998). The tumor suppressor, PTEN/MMAC1, dephosphorylates the lipid second messenger, phosphatidylinositol 3,4,5-trisphosphate. *J Biol Chem* 273, 13375-13378.

Matsumoto, K., Yokote, H., Arai, T., Maegawa, M., Tanaka, K., Fujita, Y., Shimizu, C., Hanafusa, T., Fujiwara, Y., and Nishio, K. (2008). N-Glycan fucosylation of epidermal growth factor receptor modulates receptor activity and sensitivity to epidermal growth factor receptor tyrosine kinase inhibitor. *Cancer Science* 99, 1611-1617.

Molinari, M. (2007). N-glycan structure dictates extension of protein folding or onset of disposal. *Nat Chem Biol* 3, 313-320.

Podsypanina, K., Ellenson, L.H., Nemes, A., Gu, J., Tamura, M., Yamada, K.M., Cordon-Cardo, C., Cattoretti, G., Fisher, P.E., and Parsons, R. (1999). Mutation of Pten/Mmac1 in mice causes neoplasia in multiple organ systems. *Proc Natl Acad Sci U S A* 96, 1563-1568.

Ruddock, L.W., and Molinari, M. (2006). N-glycan processing in ER quality control.

J Cell Sci 119, 4373-4380.

Samuels, Y., Wang, Z., Bardelli, A., Silliman, N., Ptak, J., Szabo, S., Yan, H., Gazdar, A., Powell, S.M., Riggins, G.J., *et al.* (2004). High Frequency of Mutations of the PIK3CA Gene in Human Cancers. *Science* 304, 554-.

Stambolic, V., Suzuki, A., de la Pompa, J.L., Brothers, G.M., Mirtsos, C., Sasaki, T., Ruland, J., Penninger, J.M., Siderovski, D.P., and Mak, T.W. (1998). Negative Regulation of PKB/Akt-Dependent Cell Survival by the Tumor Suppressor PTEN. *Science* 281, 29-39.

Stephens, L., Anderson, K., Stokoe, D., Erdjument-Bromage, H., Painter, G.F., Holmes, A.B., Gaffney, P.R., nbsp, J., Reese, C.B., *et al.* (1998). Protein Kinase B Kinases That Mediate Phosphatidylinositol 3,4,5-Trisphosphate-Dependent Activation of Protein Kinase B. *Science* 279, 710-714.

Stokoe, D., Stephens, L.R., Copeland, T., Gaffney, P.R.J., Reese, C.B., Painter, G.F., Holmes, A.B., McCormick, F., and Hawkins, P.T. (1997). Dual Role of Phosphatidylinositol-3,4,5-trisphosphate in the Activation of Protein Kinase B. *Science* 277, 567-570.

Whitman, M., Downes, C.P., Keeler, M., Keller, T., and Cantley, L. (1988). Type I phosphatidylinositol kinase makes a novel inositol phospholipid, phosphatidylinositol-3-phosphate. *Nature* 332, 644-646.

Chapter 2: Purification and characterization of ENTPD5

(This part of work was led by Dr. Min Fang. It has been accepted for publication.)

Abstract

PI3 Kinase and PTEN lipid phosphatase control the level of cellular PIP3 (Phosphatidylinositol (3, 4, 5)-trisphosphate), an activator of AKT kinase that promotes cell growth and survival. Activating mutation of PI3K and loss of PTEN are common in human cancers. We report here that an endoplasmic reticulum (ER) UDP hydrolysis enzyme, ENTPD5, is up-regulated in PTEN-null cells. *In vitro*, together with another two proteins Adenylate Kinase 1(AK1), CMPK (Cytidine/Uridine Monophosphate Kinase) and one small molecule UMP, ENTPD5 forms a futile cycle, resulting in ATP hydrolysis. *In vivo*, ENTPD5 may function as UDP hydrolysis enzyme in ER and promote protein reglucosylation.

Introduction

Activation of PI3K/AKT increases protein translation and subsequent protein glycosylation and folding in ER lumen. ER lumen has a unique calnexin/calreticulin chaperon system to facilitate folding of glycoprotein with N-linked oligosaccharides. Calnexin/calreticulin chaperon can bind only to monoglucosylated proteins. During co-translational translation, pre-synthesized dolicol-P-P-Glc3Man9GlcNAc2 was transferred to Asn residue of the protein. Three glucose moieties of the core glycan are sequentially removed by Glucosidase I and II immediately after being transferred to proteins. These deglucosylated proteins can be transiently reglucosylated on mannose

residue by UGGT (UDP-Glucose: Glycoprotein glucotransferase), resulting its binding to calnexin/calreticulin to promote their folding.

UDP is generated as a product of UDP-Glucose-dependent glycoprotein reglucosylation in the calnexin/calreticulin cycle. As an end-product, UDP inhibits activity of UGGT, a key enzyme in reglucosylation cycle (Trombetta and Helenius, 1999). For reglucosylation cycle to work, UDP-Glucose has to be transported from cytosol where it is synthesized into ER lumen where it is used by UGGT as glucose donor. The translocation of UDP-Glucose into ER lumen is via a coupled exchange with ER luminal UMP (Perez and Hirschberg, 1986; Vanstapel and Blanckaert, 1988).

Here we purified a AKT responsive ER enzyme ENTPD5 which can hydrolyze UDP to UMP. It may relieve end-product inhibition to UGGT by UDP and also promote UDP-Glucose translocation to ER lumen by providing more UMP in ER lumen.

Results and Discussion

PETN knockout MEFs have an elevated activity that hydrolyze ATP to AMP

In an attempt to study why PTEN knockout MEFs were resistant to several apoptotic stimuli in comparison to MEFs prepared from their heterozygote littermate, we prepared cytosolic extracts from these cells and studied their caspase-3 activation in vitro. As reported previously, the PTEN-null MEFs showed elevated levels of phosphorylated AKT and p70S6 kinase while the total protein level of these two kinases remained the same as in PTEN heterozygous MEFs ((Stambolic et al., 1998), Figure

2-1A). We quickly noticed that S-100 cell extracts (prepared after collecting the supernatants of 100,000 *g* span of broken cells) from PTEN-null MEFs had a reduced activity to activate caspase-3 *in vitro* compared to that from the heterozygous MEFs. Surprisingly, there was no detected difference in the level of protein components of core intrinsic apoptotic pathway including cytochrome c, Apaf-1, procaspase-9, and procaspase-3 (Li et al., 1997). The lower activity was caused by the decreased ATP level in S-100 from PTEN-null MEFs (data not shown). Adding exogenous ATP or dATP, two energy sources for caspase-9/3 activation by Apaf-1/cytochrome c, leveled the difference in caspase-3 activation between these extracts. Given that cellular ATP level is usually maintained at a rather constant level, we reasoned that the difference in ATP in S-100 was caused during the process of S-100 preparation, which took about 1 hour. Indeed, as shown in Figure 1-1B, the ATP levels in PTEN-null MEFs was only slightly lower than in the heterozygous MEFs if the measurement was carried out right after cells were harvested (columns 1-2). When the broken cell suspension, or supernatants after 10,000 *g* span (S-10), or S-100 were incubated on ice for 1 hour before the ATP levels were measured, ATP concentrations in the extracts from PTEN knockout MEFs dropped sharply while that from heterozygous MEFs declined only slightly (columns 3-8). The higher amount of ATP in S-10 extracts, we reasoned, might be released from the organelle during their preparation (column 5). These experimental data indicated that there is a higher ATP hydrolysis activity (or activities) in the PTEN knockout cell extracts. To measure such an activity directly, we incubated \square -P³²-ATP with the S-100 extracts and analyzed the radioactivity using thin layer

chromatography. As shown in Figure 1C, more radio-labeled ATP was hydrolyzed in the S-100 from PTEN knockout MEFs (lanes 4-5). Interestingly, the nucleotide was mostly hydrolyzed into AMP.

To sort out whether the observed accelerated ATP hydrolysis was due to a specific activity or a combination of non-specific ATPases, we fractionated same amount of S-100 extracts from PTEN-null and PTEN heterozygous MEFs side by side on a Q-sepharose ion-exchange column. The fractions from each column run were dialyzed and ATPase activity was measured by adding each column fraction to the S-100 from PTEN heterozygous MEF, which served as the base line activity. Surprisingly, a single peak of elevated activity centered at fractions 11-13 was observed in the fractionated S-100 from PTEN-null MEFs while much less activity was seen in these fractions from PTEN heterozygous MEFs (Figure2-1D, lanes 13-15).

ENTPD5 is responsible for the elevated ATPase activity in PTEN knockout cells

We decided to purify such an activity from large-scale cultured PTEN knockout MEFs. We took 800 milligrams of S-100 from PTEN-null MEFs and subjected it to 5 column chromatographic steps (Fig.2-2A). The ATP hydrolysis activity was measured as in Figure 2-1D and the active fractions from each column step were pooled, dialyzed, and loaded onto the next column. Finally, after a Superdex 200 gel-filtration column, the active fractions were loaded onto a Mini Q column and the protein bound to the column was eluted with a linear salt gradient and fractions were collected and assayed. Shown in Figure 2-2B, a single ATP hydrolysis peak centered at fraction 6 was

observed. When these fractions were analyzed by SDS-PAGE followed by silver staining, a protein band just below the 50-kDa molecular weight marker correlated perfectly with the activity.

This protein was then excised from the gel and subjected to mass spectrometry analysis. The identity of the enzyme turned out to be ectonucleoside triphosphate diphosphohydrolase 5, ENTPD5, a member of the enzyme family that hydrolyze tri- and/or diphospho-nucleotide to mono-phosphonucleotide (Trombetta and Helenius, 1999).

To verify that ENTPD5 is indeed the enzyme that caused higher ATP hydrolysis to AMP in PTEN-null MEFs, we first did a western blotting analysis using an antibody against mouse ENTPD5. As shown in Figure 2-2C, lower panel, ENTPD5 was only prominently detected in PTEN-null extracts (lanes 1-2). When mouse ENTPD5 was exogenously expressed in the PTEN heterozygous MEFs, the extracts from these cells showed the ability to hydrolysis to ATP to AMP just like that from PTEN-null cells (lanes 3-5). Moreover, when ENTPD5 was knocked down in PTEN-null MEFs with two different siRNA oligos, the ATP to AMP hydrolysis activity was diminished in each case while a control siRNA oligo had no effect (lanes 6-10).

To confirm that the elevated level of ENTPD5 is due to deletion of PTEN, we transfected a wild type PTEN cDNA, or the one with its phosphatase active site mutated with a C>S mutation, into PTEN-null MEFs. Indeed, restoring PTEN expression in these cells decreased phosphoAKT and diminished ENTPD5 expression while the phosphatase dead PTEN had no effect (Fig.2-2D, lanes 2-3). Consistently,

treatment of PTEN-null MEFs with a PI3 kinase inhibitor also decreased the level of ENTPD5 (Fig.2-2E, lanes 2-3).

The regulation of ENTPD5 by PI3K/AKT pathway seems to be transcriptional. Higher level of ENTPD5 mRNA was detected in PTEN-null MEFs by quantitative PCR, which was decreased to the same level as in PTEN heterozygous MEFs after treatment with a PI3 kinase inhibitor (Fig.2-2F).

UMP or GMP is a required co-factor for the ATP hydrolysis activity

During our ENTPD5 purification efforts, we noticed that a small molecule co-factor is required for the observed ATP to AMP hydrolysis activity. S-100 extracts lost such a co-factor after a dialysis procedure (Fig.2-3A, lanes 2, 4) and the activity was restored with addition of a small molecule fraction prepared by a 10-kDa cut-off filter. There was no difference in such a small molecule in PTEN heterozygous and PTEN-null MEFs (lanes 6, 8) and the molecule was even present in S-100 from HeLa cells (lane 10).

Based on its biochemical properties, we deduced that the co-factor is a nucleotide. Testing a variety of nucleotides revealed that uracil and guanine, either in tri, di, and mono-phosphate form, substituted the small molecule fraction from cells (Fig.2-3B, lanes 2-15). In contrast, thymidine nucleotides have no activity while CMP showed a slight activity.

To determine whether the conversion of UTP/UDP to UMP and GTP/GDP to GMP is necessary for the observed activity, we tested various non-hydrolysable Uracil and

fractionated HeLa cell S-100, using a Q-Sepharose column and collected both the flow through (Q-FL) and column-bound fraction eluted with 300 mM NaCl (Q-30). Either fraction alone was unable to hydrolyze ATP to AMP although Q-30 fraction, when ENTPD5 and UMP were present, hydrolyzed ATP to ADP (lanes 13-14). When the Q-FL fraction was also included, the ATP to AMP activity was fully reconstituted (lanes 18).

We then purified the activity present in the Q-30 fraction. The activity present in the Q-30 fraction was purified by subjecting HeLa S-100 onto four sequential column chromatographic steps and finally onto a Mini Q column (Fig.2-4B, left panel). The activity was eluted from this column with a linear salt gradient from 40 mM to 120 mM NaCl and fractions eluted from the column were assayed in the presence of recombinant ENTPD5, UMP, and the Q-FT fraction (Fig.2-4B, right lower panel). A peak of activity was observed at the fractions 8-10. Same fractions were subjected to SDS-PAGE followed by silver staining and two protein bands close to 37 and 20-kDa markers were correlated perfectly with the activity (Fig.2-4B, right upper panel). Both bands were identified by mass spectrometry as human UMP kinase.

The identification of UMP kinase in the Q-30 fraction shed light on why UMP is a required co-factor for the ATPase activity and how ENTPD5 plus this enzyme generates ADP from ATP. In this reaction, co-factor UMP is phosphorylated into UDP by UMP kinase and ATP, generating ADP. UDP is subsequently hydrolyzed by ENTPD5 to UMP, completing the cycle with net conversion of ATP to ADP.

With this knowledge, we then made hypothesized that the third protein factor

present in the Q flow through fraction must be Adenylate kinase that took two generated ADP and converted them to ATP and AMP therefore gave the observed ATP to AMP final outcome. To test this hypothesis, we took the Q flow through fraction and subjected it to a gel-filtration column and collected the fractions eluted from the column to assay for ATP to AMP hydrolysis in the presence of UMP, purified recombinant ENTPD5, and UMP kinase. A activity peak centered at fractions 17-18 was observed (Fig.2-4C, upper panel). When these fractions were subjected to western blotting analysis using an antibody against Adenylate kinase, the detected western blotting band correlated perfectly with the activity peak (Fig.2-4C, lower panel). The correlation held with additional chromatographic steps.

We subsequently generated recombinant UMP kinase and Adenylate kinase in bacteria and purify them to homogeneity (Fig.2-4D, lanes 9, 12). Purified recombinant ENTPD5 expressed in insect cells was running as a doublet on SDS-PAGE gel that could be shifted down after treating treatment by PNGaseF, indicating that ENTPD-5 is glycosylated.

These purified recombinant proteins allowed us to reconstitute this ATP to AMP hydrolysis cycle. Only when all three enzymes and UMP co-factor were present, efficient ATP to AMP conversion was observed (Fig.2-4D, lanes 1-8).

Discussion

Entpd5, AK1 and CMPK1/UMPK form a futile cycle *in vitro*

ENTPD5, AK1 (Adenylate Kinase) and CMPK1/UMPK form a cycle to

hydrolyze ATP *in vitro* (Figure2-5A). In one cycle, Entpd5 hydrolyzes two molecules of UDP and generates two molecules of Pi and UMP. CMPK1 converts two molecules of UMP back to UDP, and at the same time generates 2 molecules of ADP. Then Adenylate Kinase converts 2 molecules of ADP to AMP and ATP. The net reaction is hydrolyzing ATP to AMP and 2 molecules of Pi. However, in cells these enzymes are located in different compartments (AK1 and CMPK1 are in cytosol, while Entpd5 is in ER). It may need additional step for this cycle to work *in vivo*.

Analog of *in vitro* cycle and *in vivo* cycle

The ER location of ENTPD5 and its preferred specificity for UDP suggested that ENTPD5 functions in the process of reglucosylation and calnexin/calreticulin-mediated protein folding (Trombetta and Parodi, 2003). Since all ER sugar precursors are in the UDP conjugated form, UDP is generated after the conjugated sugar gets transferred to proteins. The UDP-sugars are made in cytosol and transported into ER through the UDP-sugar transport, which is an antiporter that needs to exchange out one molecule of UMP for each UDP sugar conjugate (Hirschberg et al., 1998). UDP therefore needs to be hydrolyzed to UMP to prevent end-product feedback inhibition of UGGT, as well as to provide substrate for the antiporter (Trombetta and Helenius, 1999). UMP will then be phosphorylated back to UDP by UMP kinase in cytosol and the generated ADP will be converted to ATP and AMP (diagramed in Fig.2-5B).

Materials

Cell Culture

PTEN^{+/-} and PTEN^{-/-} MEF cells were established previously (Stambolic et al., 1998) and maintained in DMEM medium supplemented with 10% fetal bovine serum (FBS) (Invitrogen) plus 200 unit/ml penicillin/streptomycin (Hyclone).

Total Cell Extracts Preparation

Cells cultures after various treatments were scraped and collected with centrifugation at 800g at 4 °C for 6 minutes, washed once with cold PBS (Invitrogen). The cell pellets were resuspended in approximately 5 times volume of buffer A (20 mM Hepes, 10 mM KCl, 1.5 mM MgCl₂, 1mM EDTA, 1 mM EGTA, 1mM DTT, 0.1 mM PMSF and complete protease inhibitor (Roche) containing 1% Triton X-100 plus Phosphatase Inhibitor I and II, vortexed for 30 seconds, set on ice for 20 minutes and followed by centrifugation at 14000 rpm at 4 °C for 15 minutes. The supernatants were collected for Western-blot analysis.

Preparation of S-100 Fractions from PTEN^{+/-} or PTEN^{-/-} MEF Cells or HeLa S3 Cells

PTEN^{+/-} and PTEN^{-/-} MEF cells were cultured in monolayer at 37 °C in an atmosphere of 5% CO₂ in DMEM medium as described above. Two days after plated, cells were scraped, harvested by centrifugation at 800g at 4 °C. After one wash with cold PBS, cell pellets were re-suspended in 5 vol of ice-cold buffer A. After sitting on ice for 20 minutes, the cells were broken by passing 22 times through a G22 needle applied onto 1 ml syringe. The resulting broken cell mixtures were centrifuged at 14000 rpm for 10 minutes. The supernatants were further centrifuged at 10⁵×g for 1

hour in a table top ultracentrifuge (Beckman). The resulting supernatant was considered S-100 fraction, stored at -80 °C and used for ATP hydrolysis assay as well as purification of Entpd5.

Suspension cultured HeLa S3 cells were obtained from Cell Culture Center in Minneapolis, MN. S-100 fraction prepared (as explained above) from HeLa S3 cells was used as source for the purification of UMP kinase and Adenylate kinase and identification of small molecule.

In Vitro ATP Hydrolysis Assay and Thin-layer Chromatography (TLC) Analysis

Aliquots of 21 μ l S-100 (1.5mg/ml) either from PTEN^{+/+} or PTEN^{-/-} MEF cells were incubated with 3 μ l 1 mM ATP, 3 μ l 0.4 μ Ci/ μ l α -P³² labeled ATP and 3 μ l 100mM MgCl₂ in total volume of 30 μ l adjusted with buffer A at 30 °C for 1 hr. Then reaction was stopped by adding 3.5 μ l 100% (W/V) trichloroacetic acid (TCA) and vortexed well followed by 10 minutes centrifugation at 14000 rpm at 4°C. Aliquots of 1 μ l resulting supernatant were spotted on TLC plate (Analtech, Cat# 105016) and dried in the air. After being overnight developing in solvent (132ml isobutyric acid plus 36 ml ddH₂O and 6 ml of 30% ammonia hydroxide), the plate was air-dried and exposed to X-ray film at room temperature for 2 hrs, or detected by phosphor-imaging in some circumstance as indicated.

Purification of Entpd5

All purification steps were carried out at 4 °C. All chromatography steps were

carried out using an automatic fast protein liquid chromatography station (Pharmacia). Eighty milliliters (0.32 g of protein) of S-100 from PTEN^{-/-} cells were prepared as described above, applied to a 10 ml SP-Sepharose HP column (Pharmacia) which was freshly equilibrated with buffer A. Flow through fraction was collected and loaded onto a 5 ml Q-Sepharose HP column (Pharmacia). The column was eluted with a linear gradient of 100 ml buffer A to buffer A containing 300 mM NaCl, followed by another 50 ml buffer A containing 1 M NaCl. Fractions of 5 ml were collected, dialyzed overnight and assayed for ATP hydrolysis activity. The active fractions (10 ml) were pooled, and ammonium sulfate was added directly to these fractions to a final concentration of 1 M. The mixture was equilibrated by rotating 3 hr at 4 °C followed by centrifugation of 35000×g for 1 hr. The resulting supernatant was loaded onto a 1 ml Phenyl-Superose column (Pharmacia) equilibrated with buffer A containing 1 M ammonium sulfate and eluted with 10 ml buffer A containing 0.5 M ammonium sulfate, then 10 ml linear gradient of buffer A containing 0.5 M ammonium sulfate to buffer A and followed by another 10 ml of buffer A. Fractions of 1 ml were collected, dialyzed overnight and assayed for ATP hydrolysis activity. 3 ml of active fractions were pooled, concentrated by using spin column (Amicon® Ultra) to 1 ml and loaded in two separate runs on a Superdex 200 (10/30) gel filtration column equilibrated with buffer A containing 50 mM NaCl. The column was eluted with same buffer. Fractions of 1 ml were collected and assayed for ATP hydrolysis activity. A total of 4 ml active fractions were pooled and loaded on a Mini Q (Pharmacia) column. The column was washed with 1 ml buffer A and eluted with 1ml

buffer A containing 100 mM NaCl followed by another 2 ml linear gradient of 100 mM NaCl to 150 mM NaCl, both in buffer A. Fractions of 100 μ l were collected and assayed for ATP hydrolysis activity. Active fractions were aliquoted with addition of 10% glycerol and stored at -80°C.

Purification of UMP Kinase

160 ml S-100 (0.8 g of protein) from HeLa S3 cells were prepared as described above and applied to a 10 ml Q-Sepharose HP column (Pharmacia) equilibrated with buffer A. The column was eluted with a 200 ml linear gradient of buffer A to buffer A containing 200 mM NaCl followed by another 100 ml buffer A containing 1 M NaCl. Fractions of 10 ml were collected and dialyzed against buffer A overnight at 4 °C, assayed for ATP hydrolysis activity. Active fractions (20 ml) were pooled, dialyzed, and passed through 1 ml SP-Sepharose HP column (Pharmacia). Flow through fraction was collected and directly loaded on a 1ml Heparin HP column (Pharmacia). After washing with five column volume of buffer A, the column was eluted with 20 ml linear gradient of buffer A to buffer A containing 600 mM NaCl. Fractions of 1 ml were collected, dialyzed against buffer A overnight at 4 °C and assayed for ATP hydrolysis activity. Active fractions were pooled and loaded in 8 separate runs on Superdex 200 (10/30) (Pharmacia) equilibrated with buffer A containing 50 mM NaCl. The column was eluted with same buffer. Fractions of 1 ml were collected and assayed for ATP hydrolysis activity. A total of 16 ml of active fractions were pooled and loaded on Mini Q column. The column was eluted with 2 ml linear gradient of

buffer A to buffer A containing 200 mM NaCl. Fractions of 100 μ l were collected for ATP hydrolysis activity assay and silver staining immediately.

Small Molecular Recovery from S-100 Fraction

S-100 fractions from PTEN^{+/-}, PTEN^{-/-} MEF cells or HeLa S3 cells were obtained as described above. 2 ml of S-100 were applied to 2 ml spin column (10K cut Centrifugal filter devices) (Centricon, Cat№ 4205). The columns were centrifuged at 10000 rpm in JA-21 Centrifuge (Beckman) according to manufacturer's protocol. 1.8 ml of solution was centrifuged down to bottom vial of the column and used as source for identification of small molecule.

Plasmids and siRNA Oligoes

Human and mouse siRNA against Entpd5 were from Dharmacon ON-TARGET plus siRNA pools of four oligoes. ihEntpd5D3 (5'-CAU AUU AGC UUG GGU UAC UUU-3'), ihEntpd5D4 (5'-CGA GAU GGU UGG AAG CAG AUU-3'), imEntpd5D1 (5'-GGA CAU ACG UUU CGA AGU GUU-3'), imEntpd5D2 (5'-GGA AAA GCC UGG CCC GAA AUU-3') and control siRNA iGFP (5'- CUG GAG UUG UCC CAA UUC CUU-3') were synthesized by Dharmacon.

Preparation of Recombinant Entpd5, UMPK and Adenylate Kinase

Human Entpd5 recombinant protein was generated using Bac-to-Bac Baculovirus Expression Systems (Invitrogen Cat# 10359-016). Full-length human Entpd5 cDNA

was cloned into pFastBac1 with C-terminal-fused 6xHis and FLAG double tags. Baculovirus was produced and amplified to 2×10^9 pfu/ml following manufacturer's instructions. SF9 cells were grown to 2×10^6 cells/ml in SFM 900 II media (Invitrogen Cat# 10902096), and then infected with Entpd5 expressing baculovirus at Multiplicity of Infection (MOI) of 4. After 72hr of infection, cells were harvested and homogenized in buffer A by douncing as described previously (Zou et al., 1999). The recombinant protein was purified using Ni-NTA agrose beads (Qiagen Cat#30230) following manufacturer's protocol.

Human UMPK and human adenylate kinase cDNA were cloned into pET21a (Novagen Cat#69740-3), with C-terminal 6His tag. BL21DE3 bacteria was transformed and grown at 37°C to an OD600 of about 0.6. Then the bacteria culture was switched to 20°C, and recombinant protein expression was induced by 0.2mM IPTG for overnight. Bacteria were harvested and lysed by sonication, and the recombinant proteins were purified following standard Ni-NTA purification protocols.

Generation of Stable Cell Lines

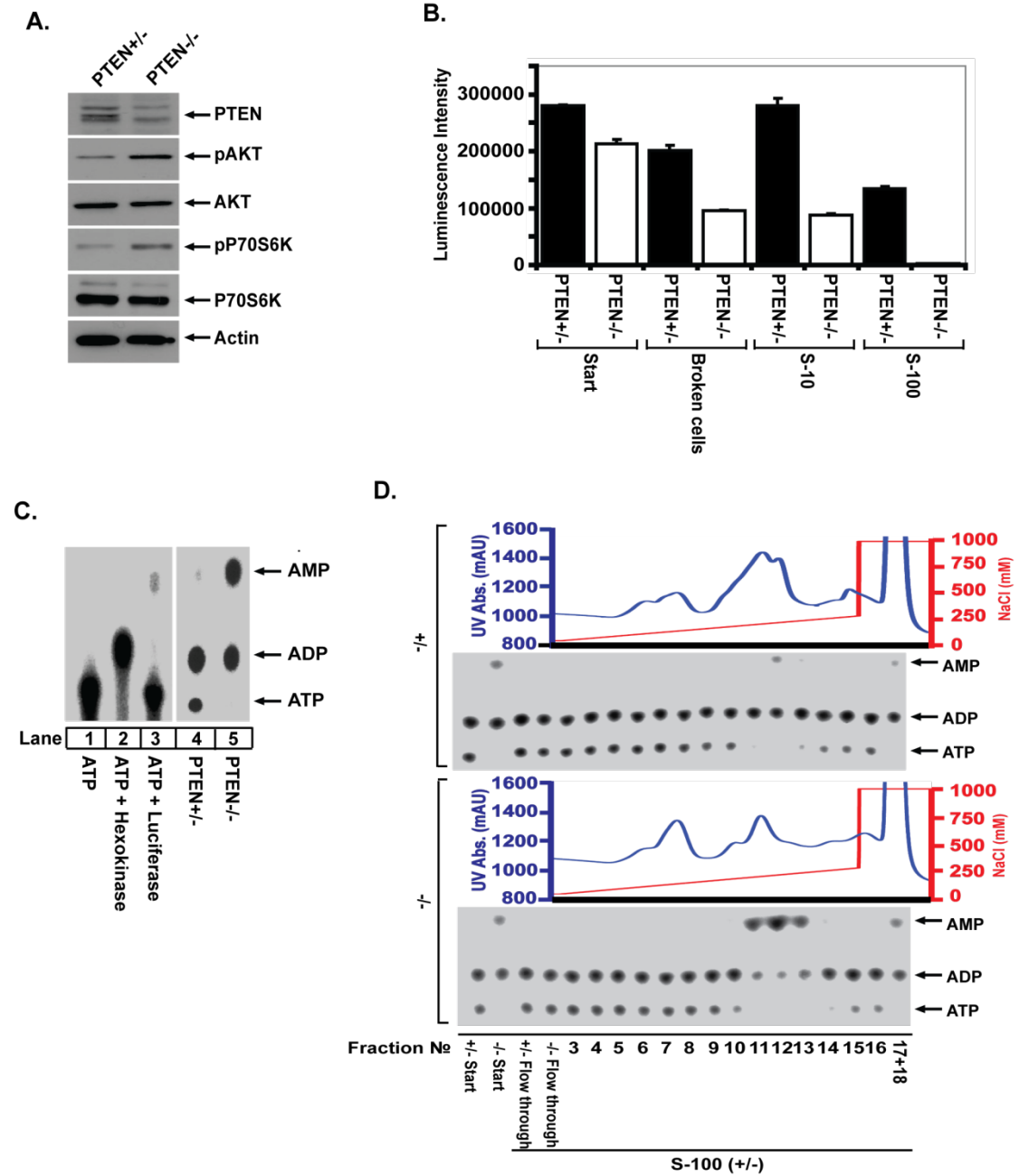
To Generate Entpd5 overexpression cells, 4 μ g of expression plasmids containing mouse Entpd5 were transfected into PTEN \pm MEF cells using Lipofectamin 2000 (Invitrogen) according protocol provided by manufacturer. Twenty-four hours post transfection, cell were split at 1 to 30 dilution and selected by addition of 0.6 mg/ml Hygromycin in complete DMEM medium for 3 weeks. Clones were lifted and tested for expression of transgene by western blot analysis.

For establishment of tetracycline repressor expression cells, an expression plasmid containing tetracycline repressor (TetR) was transfected into either PTEN^{-/-} MEF cells or LNCaP cells as described above and selected by 15 or 10 µg/ml blasticidine respectively. Inducible mouse or human Entpd5 shRNA construct was then stably introduced into PTEN^{-/-} TetR or LNCaP TetR cells, selected with 2 or 0.25 µg/ml puromycin respectively. Finally, wild-type or catalytic dead version of Entpd5 rescue cells were generated by transfecting either PTEN^{-/-} Entpd5 shRNA cells or LNCaP Entpd5 shRNA cells with mouse or human shRNA resistant Entpd5 expression constructs and selected with 0.8 mg/ml Hygromycin or 0.5 mg/ml G418 respectively. To maintain transgene expression, all the stable cell lines were cultured in complete medium supplemented with various antibiotics as indicated.

Quantitative PCR Analysis

Total RNA from PTEN^{+/-} and PTEN^{-/-} MEF cells was extracted by the Trizol reagent (Invitrogen). One microgram of total RNA was used for first strand cDNA synthesis with superscript reverse transcriptase (RT) (Invitrogen). Real-time quantitative PCR was performed by the fluorescent dye SYBR Green methodology using Power SYBR Green PCR kit (Applied Biosystems) and the 7900 HT Fast Real-Time PCR System (Applied Biosystems). Primer pairs for target gene were chosen with the Primers Express software (Applied Biosystem): ENTPD5, sens 5'-ATGACCCTGCCTCCACAGGAGTGTGAGCAG-3', antisens 5'-GCCTGGGCTTTCTGCTCAGGCAGCAAACG-3' 18S, sens 5'-GCC TGAGAAACGGCTACCA-3', antisens 5'-GTCGGGAGTGGGTAATTTGC-3'.

Briefly, cDNA was mixed with 25 μ l Master Mix containing 10 reaction buffer, 25 mM MgCl₂, 2.5 mM dNTP, 300 nM of each primer, 0.025 U/ μ l AmpliTaq Gold® DNA Polymerase and 0.75 μ l of 1/2000 diluted SYBR green stock in a final volume of 50 μ l. A first step of 10 min at 95 °C was followed by 40 cycles of amplification (95 °C for 15 s and 60 °C for 60 s). Using the comparative Ct method, the amount of entpd5 mRNA was normalized to the 18S amount.



AKT, phosphorylated P70S6 kinase (pP70S6K), P70S6 kinase, and β -actin expression levels respectively.

(B) Higher level of ATP hydrolysis in PTEN^{-/-} MEF cells during preparation of cell lysates compared with PTEN^{+/-} MEF cells. PTEN^{+/-} and PTEN^{-/-} cells (1×10^7) were harvested by 800g centrifugation at 4°C and cell lysates (S-100 fractions) were prepared as described in Experimental Procedures. On each step of preparation, aliquots of 20 μ l samples were incubated on ice for 1 hour and then diluted 25 times followed by immediate measurement of ATP by Cell Titer-Glo kit (see Experimental Procedures for details).

(C) PTEN^{-/-} cell lysate hydrolyzes ATP to AMP. Lane 4 and 5, Cell lysates (S-100 fraction) from PTEN^{+/-} and PTEN^{-/-} cells were normalized to 1.5 mg/ml, ATP hydrolysis assay was performed as described in Experimental Procedures. Lane 1-3, ATP, ADP and AMP positive controls: mixture of 4 μ Ci α -P³² labeled ATP with buffer A (ATP) (lane 1) or with 20 mM sucrose (final concentration) plus 0.1 unit hexokinase (ADP) (lane 2), or with 20 μ l Cell Titer-Glo reagent (AMP) (lane 3) in total volume of 100 μ l were incubated at 30°C for 1 hour. After incubation, the reaction was stop by boiling at 95°C for 15 minutes, small molecule was recovered by 10K cut spin column (Amicon® Ultra, Ca №: UFC501096). 1 μ l of samples were loaded onto TLC plate. After overnight developing, the plate was air-dried and exposed to X-ray film for 2 hours at room temperature. Positions for ATP, ADP or AMP were indicated.

(D) One protein peak difference between PTEN^{+/-} and PTEN^{-/-} cell lysates cause

high level of ATP hydrolysis in PTEN^{-/-} MEF cell lysates. 6 ml of S-100 from PTEN^{+/-} and PTEN^{-/-} cells (3.5 mg/ml) were loaded onto 1 ml Q-sepharose HP column, after equilibrated with buffer A, the column was eluted with linear gradient of 16 ml buffer A to buffer A containing 250 mM NaCl followed by another 5 ml of buffer A containing 1M NaCl. Fractions of 1 ml were collected and dialyzed overnight at 4°C. 10.5 µl of each fraction was mixed with another 10.5 µl of un-dialyzed S-100 from PTEN^{+/-} cells, assayed for ATP hydrolysis activity as described in Experimental Procedures (lower panels, positions of ATP, ADP and AMP were indicated in the right). FPLC histograms were presented at upper panels respectively.

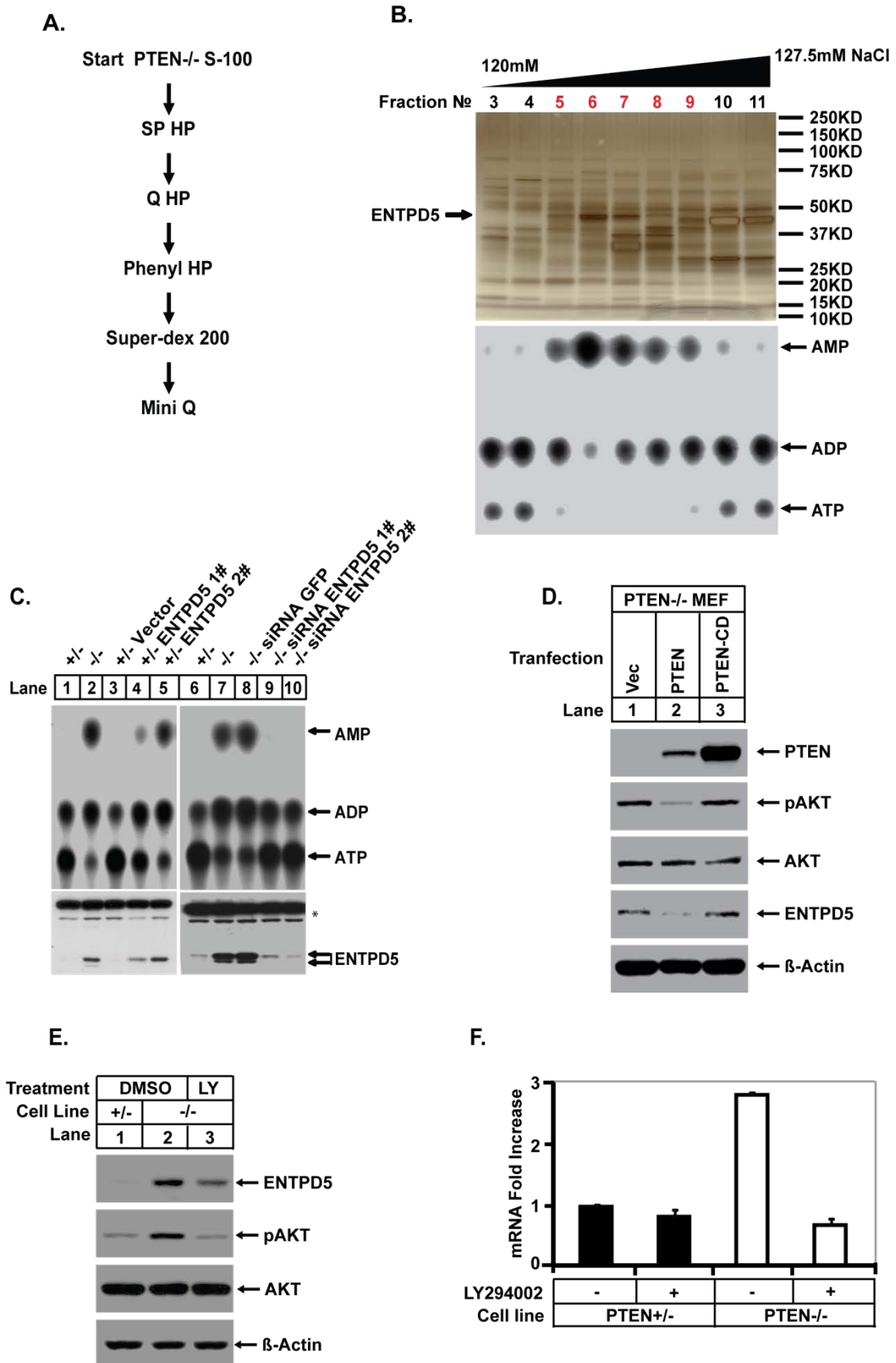


Figure 2-2. Purification of Entpd5 and Its Regulation by PTEN-AKT Signaling

Pathway

(A) Diagram of the purification scheme for ATP hydrolysis activity in PTEN^{-/-} MEF cell. See Experimental Procedures for details.

(B) Final step of purification. Upper: aliquots of 30 μ l of indicated fractions were subjected to 4-10% gradient SDS-PAGE gels (Invitrogen) followed by staining using a Silver Staining kit from Invitrogen. Lower: Aliquots of 3 μ l of indicated fractions were incubated with 10.5 μ l of un-dialyzed S-100 from PTEN^{+/-} MEF cells, 3 μ l of α -P³² labeled ATP (0.4 μ Ci/ μ l), 3 μ l ATP (1 mM), 3 μ l MgCl₂ (100mM) in a total volume of 30 μ l adjusted with buffer A at 30°C for 1 hour. After incubation, radioactive ATP, ADP and AMP were visualized by Thin-layer Chromatography (TLC) as described in Experimental Procedures.

(C) Confirm of Entpd5 purification in vivo. Lane 1 to 5, gain of ATP hydrolysis activity in PTEN^{+/-} MEF cell by stable expression of Entpd5. PTEN^{+/-} Vec or PTEN^{+/-} Entpd5 1# and 2# (two individual clone with different expression level of Entpd5) were established as described in Experimental Procedures. Cell lysates (S-100) from indicated cell lines were prepared and normalized to 1.5 mg/ml, 21 μ l of samples were mixed with 3 μ l of α -P³² labeled ATP (0.4 μ Ci/ μ l), 3 μ l ATP (1mM), 3 μ l MgCl₂ (100mM) and assayed for ATP hydrolysis activity. Lane 6 to 10, loss of ATP hydrolysis activity in PTEN^{-/-} MEF cells by transiently knocking down Entpd5. On day 0, PTEN^{+/-} and PTEN^{-/-} cells were seeded at density of 10x10⁴ cells/100 mm dish in DMEM medium without antibiotics, on day 1, PTEN^{-/-} cells were either left un-transfected (lane 6 and 7) or transfected with 20 μ l siRNA oligo (20 μ M) against

GFP (lane 8), Entpd5 (lane 9 and 10, two different oligoes respectively), on day 3, medium in the dishes were replaced with fresh regular DMEM medium, on day 5 cells were harvested and cell lysates (S-100 fraction) were prepared, normalized to 1.5 mg/ml and assayed for ATP hydrolysis activity as described in Experimental Procedures. Upper panel: ATP hydrolysis activity resolved by ascending thin-layer chromatography. Position of ATP, ADP and AMP are indicated. Lower panel: Aliquots of 10 µg protein of indicated samples were subjected to 10% SDS-PAGE, followed by western analysis of Enptd5 to verify the Entpd5 expression level (lane 1 to 5) and knocking down efficiency (lane 6 to 10). Asterisk denotes none specific cross reactive proteins with Enptd5 antibody.

(D) Wild type PTEN but not PTENcs, catalytic dead mutated PTEN, decreases Entpd5 expression in PTEN^{-/-} cells. On day 0, PTEN^{-/-} MEF cells were seeded at density of 50×10^4 cells/100 mm dish in DMEM without antibiotics, on day 1, each 100mm dish cells was transfected with 4 µg plasmid DNA containing vector control (lane 1) or PTEN (lane 2) or PTENcs (lane 3). 24 hours after transfection, cells were harvested and total cell lysates were prepared. Aliquots of 10 µg of protein were loaded onto 10% SDS-PAGE followed by western analysis of levels of PTEN, AKT, phosphorylated AKT(pAKT), Entpd5 and β-actin as indicated.

(E) Inhibition of PI3 kinase activity decreased Entpd5 protein expression. PTEN^{+/-} and PTEN^{-/-} MEF cells were treated with DMSO or LY294002 (50 µM) for 24 hours. Total cell extracts were prepared as described in Experimental Procedures. Aliquots of 20 µg protein were subjected to 10% SDS-PAGE followed by western analysis using

indicated antibody.

(F) Inhibition of PI3 kinase decreases Entpd5 mRNA level. PTEN^{+/-} and PTEN^{-/-} MEF cells were treated with DMSO or LY294002 (50 μ M) for 48 hours and total RNA was prepared. Entpd5 mRNA level was quantified by Real-Time PCR normalized to 18s mRNA as described in Experimental Procedures.

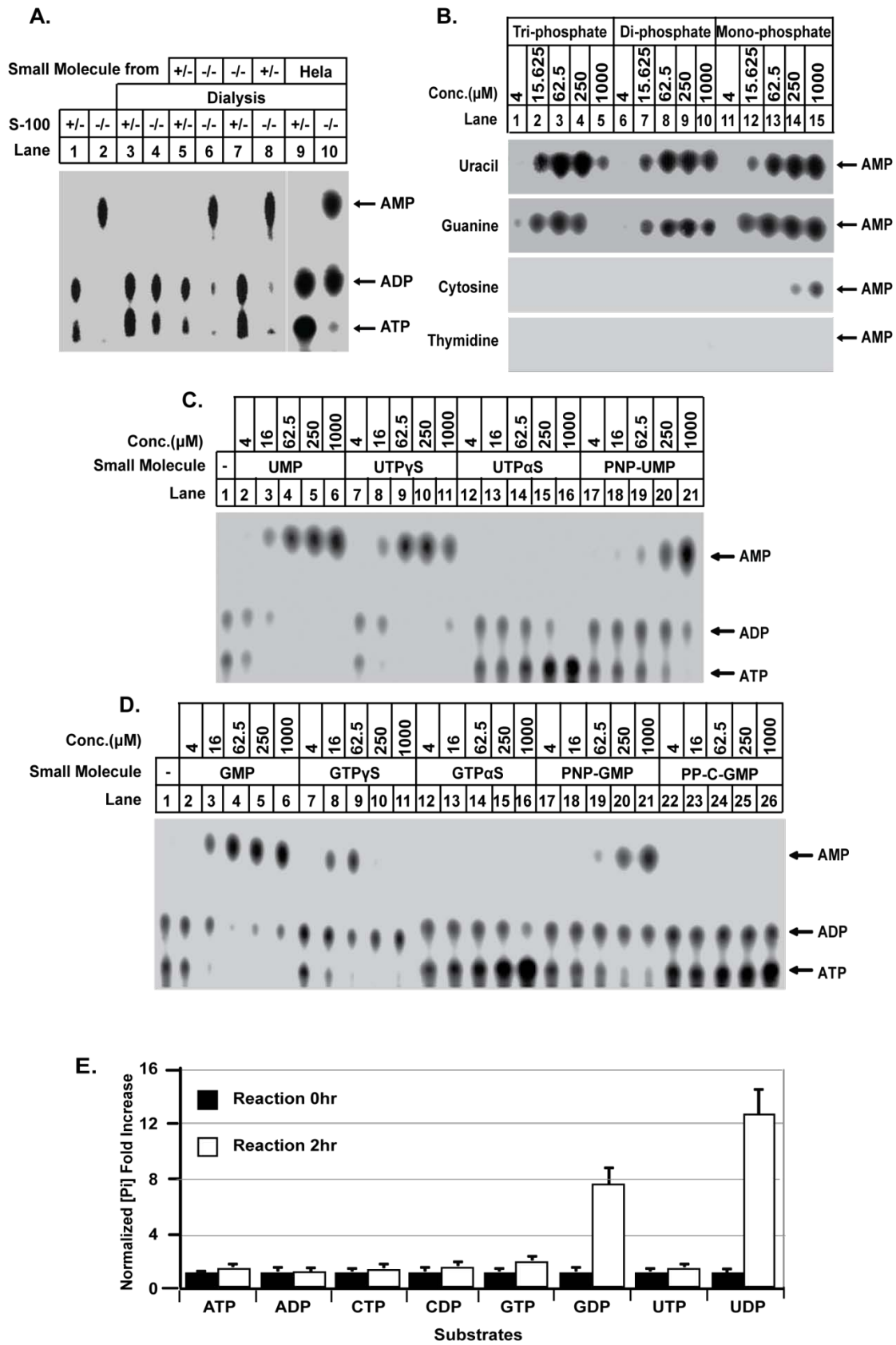


Figure 2-3. Small Molecule Requirement for Entpd5 Mediated ATP Hydrolysis and Its Identification.

(A) Small molecule is required for ATP hydrolysis activity in PTEN^{-/-} MEF cells.

Small molecule was extracted either from PTEN^{+/-} or PTEN^{-/-} MEF cells or HeLa S3 cell lysates (S-100 fractions) as described in Experimental Procedures. Aliquots of 10.5 μ l un-dialyzed cell lysates (lane 1 and 2) or dialyzed cell lysates (lane 3 to 10) from PTEN^{+/-} (lane 1, 3, 5, 7, 9) or PTEN^{-/-} (lane 2, 4, 6, 8, 10) MEF cells (3.5 mg/ml) were mixed with another 10.5 μ l buffer A (lane 1 to 4) or small molecule recovered from PTEN^{+/-} (lane 5 and 8), PTEN^{-/-} cells (lane 6 and 7) or from HeLa S3 cells (lane 9 and 10) and assayed for ATP hydrolyzing activity. Thin-layer chromatography (TLC) was performed to visualize radioactive ATP, ADP and AMP.

(B) Uracil and guanine nucleotides have ATP hydrolysis activity. Aliquots of 10.5 μ l dialyzed S-100 from PTEN^{-/-} MEF cells (3.5 mg/ml) were incubate in the presence of indicated final concentration of UTP, UDP and UMP (first panel) or GTP, GDP and GMP (second panel) or CTP, CDP and CMP (third panel) or TTP, TDP and TMP (fourth panel) at 30°C with 3 μ l of α -P³² labeled ATP (0.4 μ Ci/ μ l), 3 μ l ATP (1 mM), 3 μ l MgCl₂ (100 mM) in total volume of 30 μ l at 30°C for 1 hour followed by TLC to resolve hydrolyzed radioactive AMP. Position of AMP on TLC plate is indicated.

(C) Conversion of UTP, UDP to UMP is required for ATP hydrolysis activity in PTEN^{-/-} cell lysates. Aliquots of 10.5 μ l of dialyzed S-100 prepared from PTEN^{-/-} MEF cells were mixed with buffer A (lane 1) or indicated final concentration of UMP (lane 2 to 6), UTP γ S (lane 7 to 11), UTP α S (lane 12 to 16), PNP-UMP (lane 17 to 21) and assayed for ATP hydrolysis activity. The radioactive samples were resolved by TLC. Positions of radioactive ATP, ADP and AMP are indicated.

(D) Conversion of GTP, GDP to GMP is required for ATP hydrolysis activity in PTEN^{-/-} cell lysates. Same as in panel C, aliquots of 10.5 μ l of dialyzed S-100 prepared from PTEN^{-/-} MEF cells were mixed with buffer A (lane1) or indicated final concentration of GMP (lane 2 to 6), GTP γ S (lane 7 to 11), GTP α S (lane 12 to 16), PNP-GMP (lane 17 to 21), PP-C-GMP (lane 22 to 26) and assayed for ATP hydrolysis activity. The radioactive samples were resolved by TLC. Positions of radioactive ATP, ADP and AMP are indicated.

(E) Substrate specificity of recombinant Entpd5. The reaction was carried out in triplicate by mixing 0.1 mg/ml Entpd5 recombinant protein with 50mM of indicated nucleotides in buffer A with additional 10 mM MgCl₂. After 2hr incubation at 30°C, released free phosphate was measured by Malachite Green Assay (See Experimental Procedures for details). Data shown is representative of three independent experiments. Error bars indicate SEM.

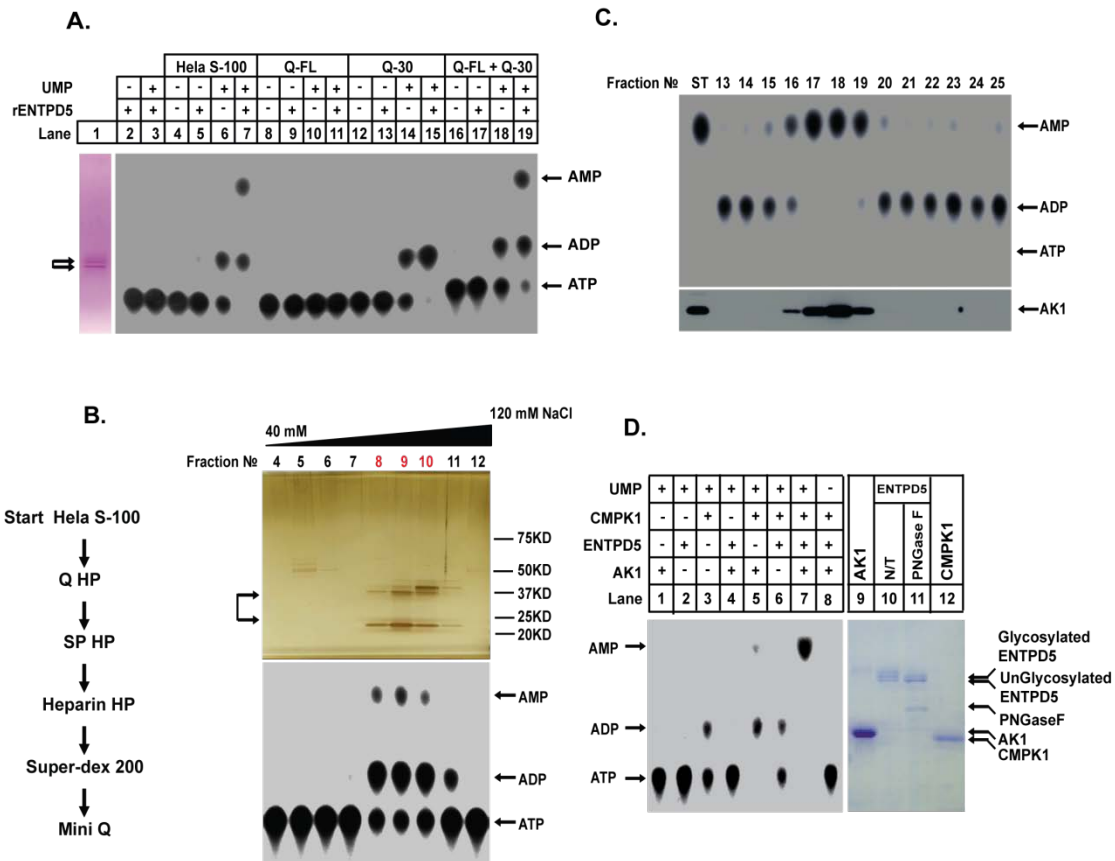


Figure 2-4. Total Reconstitution of Entpd5 Mediated ATP hydrolysis Activity in Vitro by Recombinant Entpd5, UMP and Two Additional Factors UMP Kinase and Adenylate Kinase

(A) Two additional factors are required for mediated ATP hydrolysis activity. Lane1, an aliquot of 120 ng (20 μ l) recombinant Entpd5 were subjected to 10% SDS-PAGE, the gel was subsequently stained by Coomassie brilliant blue. Arrows indicate recombinant Entpd5. HeLa S3 cell S-100 (3.5 mg/ml) was prepared and fractionated by Q-sepharose column to 2 fractions (Q FL [flow through] and Q30). Q30 represents fraction eluted with buffer A containing 300 mM NaCl. These two fractions and starting material (HeLa S-100) were dialyzed against buffer A overnight at 4°C. Aliquots of 15 μ l buffer A (lane 2 and 3) or dialyzed HeLa cell S-100 (lane 4 to 7), Q FL (lane 8 to 11), Q30 (lane 12 to 15) or Q FL combined with Q 30 (7.5 μ l each) (lane

16 to 19) were mixed with (lane 2, 3, 5, 7, 9, 11, 13, 15, 17, 19) or without (lane 4, 6, 8, 10, 12, 14, 16, 18) indicated amount of recombinant Entpd5 in the presence (lane 3, 6, 7, 10, 11, 14, 15, 18, 19) or absence (lane 2, 4, 5, 8, 9, 12, 13, 16, 17) of 100 μ M UMP (final concentration) in total volume of 30 μ l adjusted with buffer A and assayed for ATP hydrolysis activity. Radioactive sample were resolved by TLC as described in Experimental Procedures. Positions of radioactive ATP, ADP and AMP are indicated.

(B) Purification of UMP kinase in Q30 fraction. Left panel: diagram of the purification scheme for the required factor in Q30. See Experimental Procedures for details. Right panel: final step of purification of UMP kinase. Upper, Aliquots of 60 μ l indicated Mini Q fractions were subjected to 4-10% gradient SDS-PAGE followed by silver staining using Silver Stain kit from Invitrogen. Arrow indicates the protein band correlated with ATP hydrolysis activity. Lower, Aliquots of 5 μ l indicated fractions were mixed with 15 μ l of dialyzed Q FL fraction in the presence of 100 μ M UMP (final concentration) and 18 ng recombinant Entpd5 in total volume of 30 μ l, assayed for ATP hydrolysis activity. After 1 hour incubation at 30°C, TLC was performed to visualize radioactive ATP, ADP and AMP. Positions of radioactive ATP, ADP and AMP are indicated.

(C) Another required factor in Q FL fraction is correlated with Adenylate kinase on Gel-filtration column. An aliquot of 3 ml Q FL fraction from Hela cell S-100 was concentrated to 600 μ l with spin column (Amicon® Ultra, Ca №: UFC501096) following instruction provided by the manufacturer. An aliquot of 500 μ l concentrated QFL was load onto 25 ml Supdex-200 column (10/30) and eluted with buffer A

containing 50 mM NaCl. Fractions of 1 ml were collected and aliquots of 7.5 μ l of indicated fractions were combined with 7.5 μ l dialyzed Q30 fraction from HeLa cell S-100, 100 μ M UMP and 18 ng of recombinant Entpd5 in total volume of 30 μ l adjusted with buffer A, assayed for ATP hydrolysis activity. Upper panel, TLC plate resolves hydrolyzed radioactive ADP and AMP. Positions of radioactive ATP, ADP and AMP are indicated. Lower panel, aliquots of 10 μ l of indicated fractions were subjected to 10% SDS-PAGE and transferred to nitrocellulose filter. Western analysis was performed to visualize Adenylate Kinase 1 level in indicated fractions.

(D) Total reconstitution of Entpd5 mediated ATP hydrolysis by recombinant Entpd5, UMP Kinase, Adenylate Kinase and UMP. Left, aliquots of recombinant Adenylate kinase (lane 1), Entpd5 (lane 2) and UMP kinase (lane 3) (final concentration, 1 μ g/ml) were incubated alone or sequentially combined each two at a time as indicated (lane 4 to 6) or three together (lane 7 and 8) in the presence (lane 1 to 7) or absence (lane 8) of UMP (100 μ M) with 3 μ l α -P³² labeled ATP (0.4 μ Ci/ μ l) and 3 μ l ATP (1 mM) and 3 μ l MgCl₂ (100 mM) in total volume of 30 μ l at 30°C for 1 hour. After incubation, TLC was performed to visualize hydrolyzed radioactive nucleotides. Position of ATP, ADP or AMP was indicated. Right, aliquots of 10 μ g recombinant Adenylate kinase (lane 9), Entpd5 (lane 10) or Entpd5 pre-treat with PNGase F (NEB) (50 units/ μ g Entpd5) (lane 11) and UMP kinase (lane 12) were subjected to 10% SDS-PAGE followed by Coomassie brilliant blue staining.

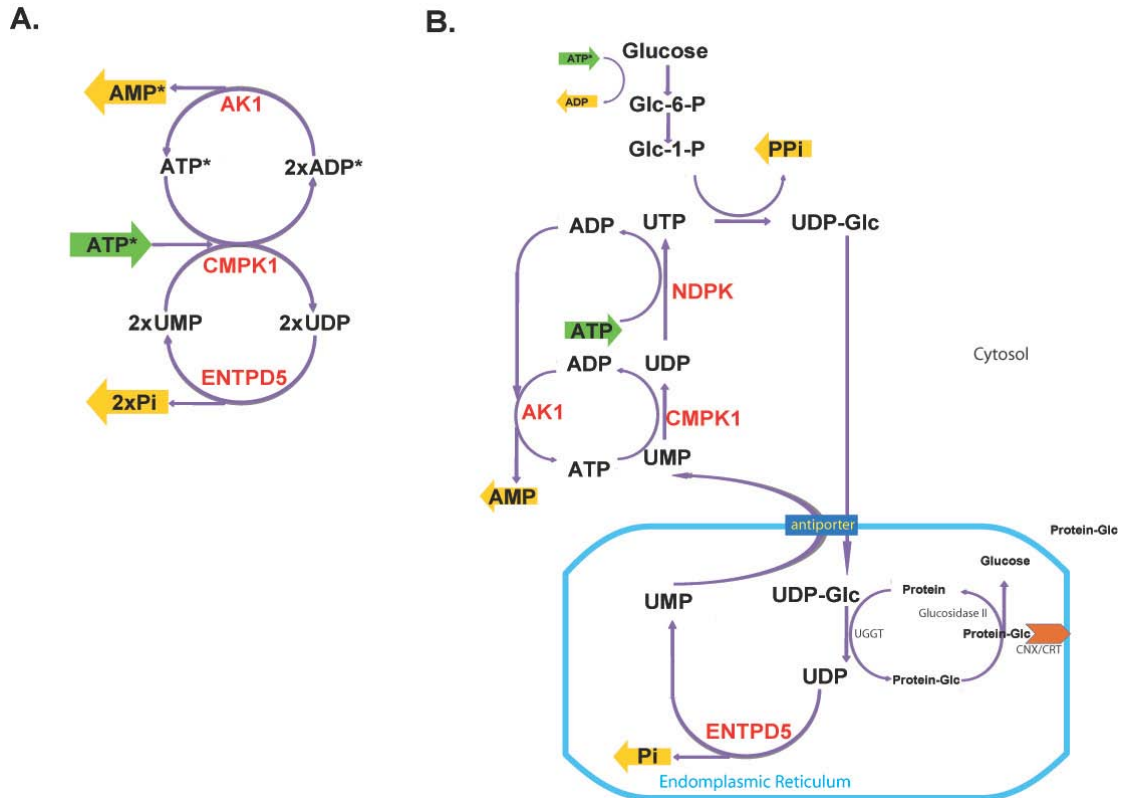


Figure 2-5 Working model for Entpd5 in vitro and in vivo

(A.) Entpd5 forms a in vitro futile cycle with UMP Kinase(CMPK1/UMPK) and Adenylate Kinase(AK1) to hydrolyze ATP.

(B.) Entpd5 is located in ER and may relieve inhibition of UDP to protein folding cycle by hydrolyzing UDP, end-product of protein reglucosylation reaction. In this process, the system uses ATP as energy to drive protein folding cycle and facilitate protein folding.

Reference:

Hirschberg, C.B., Robbins, P.W., and Abeijon, C. (1998). Transporters of nucleotide sugars, ATP, and nucleotide sulfate in the endoplasmic reticulum and Golgi apparatus. *Annu Rev Biochem* 67, 49-69.

Li, P., Nijhawan, D., Budihardjo, I., Srinivasula, S.M., Ahmad, M., Alnemri, E.S., and Wang, X. (1997). Cytochrome c and dATP-dependent formation of Apaf-1/caspase-9 complex initiates an apoptotic protease cascade. *Cell* 91, 479-489.

Perez, M., and Hirschberg, C.B. (1986). Topography of glycosylation reactions in the rough endoplasmic reticulum membrane. *J Biol Chem* 261, 6822-6830.

Stambolic, V., Suzuki, A., de la Pompa, J.L., Brothers, G.M., Mirtsos, C., Sasaki, T., Ruland, J., Penninger, J.M., Siderovski, D.P., and Mak, T.W. (1998). Negative regulation of PKB/Akt-dependent cell survival by the tumor suppressor PTEN. *Cell* 95, 29-39.

Trombetta, E.S., and Helenius, A. (1999). Glycoprotein reglucosylation and nucleotide sugar utilization in the secretory pathway: identification of a nucleoside diphosphatase in the endoplasmic reticulum. *EMBO J* 18, 3282-3292.

Trombetta, E.S., and Parodi, A.J. (2003). Quality control and protein folding in the secretory pathway. *Annu Rev Cell Dev Biol* 19, 649-676.

Vanstapel, F., and Blanckaert, N. (1988). Carrier-mediated translocation of uridine diphosphate glucose into the lumen of endoplasmic reticulum-derived vesicles from rat liver. *The Journal of Clinical Investigation* 82, 1113-1122.

Zou, H., Li, Y., Liu, X., and Wang, X. (1999). An APAF-1/cytochrome c multimeric

complex is a functional apoptosome that activates procaspase-9. *J Biol Chem* 274, 11549-11556.

Chapter 3: Regulation of Entpd5 by PI3K/AKT signaling pathway

Abstract

In previous chapter, we found that Entpd5 is regulated by PI3 Kinase pathway. Here we further characterized how Entpd5 is regulated and its correlation with AKT activation in prostate tumor samples. We showed that Entpd5 is regulated by PI3 kinase pathway through FoxO family members in cancer cell lines.

Introduction:

In many cancer cells, PTEN is often deleted or mutated. Loss of PTEN allows accumulation of PIP3 and therefore activation of downstream AKT. The downstream targets of AKT include Forkhead transcription factors (FoxO), which are FoxO1, FoxO3 and FoxO4. Phosphorylation of FoxO transcription factors by AKT induces binding to scaffold protein 14-3-3, resulting translocation of FoxOs to cytosol and inhibition of their function as transcription factors (Biggs et al., 1999; Brunet et al., 1999). Decreased expression of FoxO family members is associated with cancer progression (Fei et al., 2009; Lynch et al., 2005). Expression of Foxo3a suppresses proliferation and tumorigenesis of PTEN null cancers (Shiota et al., 2010; Zou et al., 2008).

FoxOs can induce apoptosis and cell cycle arrest by up-regulating target genes such as p27kip, FasL and Bim(Lam et al., 2006), or down-regulating cyclin D1 and cyclin D2 in different conditions(Fernandez de Mattos et al., 2004). FoxO family

members can act as an transcription activator or transcription repressor by binding to their consensus sequence TTGTTT(T/A/C).

In the present study, we demonstrated that FoxO transcription factor could repress Entpd5 expression via binding to the Entpd5 promoter region. This suggests that activation of PI3K/AKT pathway, may relieve inhibition of Entpd5 by FoxO family members.

Results:

Regulation of Entpd5 by PI3K/Akt signaling pathway through FoxO family transcription factor

In the previous study, we found the entpd5 is regulated by PI3K/AKT signaling pathway at transcriptional level. Using entpd5 promoter controlled Luciferase reporter, we further confirmed that this promoter activity is positively regulated by PI3K signaling pathway as chemical inhibition of activation of PI3K by 10uM PI3K inhibitor LY29400 attenuated promoter activity (Figure4-1A).

To identify which transcription factor mediates the effect of AKT/PI3K, we analyzed upstream regulatory sequence using bioinformatics analysis. We indentified a panel of potential TFBS (transcription factor binding sites) by searching entpd5 upstream 1kb promoter region in TRANSFAC database using MATCH program(Kel et al., 2003). Comparative genomics analysis showed that several FoxO binding sites are conserved between human and mouse (Figure4-1B). Some of the sites are

identical to the FoxO consensus site (Figure4-1B). The binding abilities of these sequences are assessed by gel shift assay using biotin-labeled DNA probes. The predicted FoxO binding sequences can bind to FoxO while mutation in the key site of binding sequence abolished binding between probe and FoxO protein (Figure4-2A, Lane 10 versus Lane 3).

To further examine effects of FoxO on *entpd5 in vivo*, we co-transfected FoxO family expression vectors with luciferase reporter gene construct containing the upstream 1kb promoter (*hentpd5-pro-Luc*) into 293T cells. As shown in Fig4-2B, all FoxO family members (FoxO1-4) suppressed *Entpd5* promoter activity. In addition, the binding of FoxOs to *entpd5* promoter were further analyzed using Chromatin-IP assay. Binding to *entpd5* promoter was increased after LNCaP cells were treated with PI3K inhibitor LY294002 (Figure4-2C).

Microarray data analysis revealed correlation of expression of *Entpd5* with activation of RTK/PI3K signaling pathway

It would be very important to determine whether *Entpd5* is also over-expressed in tumors and whether expression of *Entpd5* is correlated with activation of PI3K signaling pathway, since our previous study on function and regulation of *Entpd5* is mostly done in cell culture and mouse model. Since microarray data of many cancer cell lines and tumors are publicly available, it would be very interesting to examine expression of *Entpd5* in tumor samples from cancer patients. By analyzing a group of

recently publicized microarray data (Bermudo et al., 2008), we found that Entpd5 is highly expressed in all 20 tumor samples from cancer patients compared to normal prostate epithelium cells(Figure4-3 A).

Co-regulated genes usually have similar function or act in the same cellular pathway, and therefore examination of co-regulated genes will shed more insight on the function or regulation of uncharacterized genes. After clustering all gene expression profile from prostate tumor microarray data using SOM (Self-Organization Method), we identified dozens of genes that are significantly co-regulated with Entpd5. Expression of these genes indicates that these tumor samples have high AKT activation. As shown in Fig 5-3, many of these genes are involved in activating RTK signaling (HER-3, PI3KCB, EGF), downstream PI3K (S6Kinase and Ras) and transcription target genes (CD36(van Oort et al., 2008), IL8(Tong et al., 2008) and Osteopontin(Packer et al., 2006))(Figure4-3 A). Although it is hard to directly measure activity of PI3K, these highly expressed components of RTK signaling suggest that these tumor samples have high activation of RTK signaling. By comparing normalized Entpd5 signal with signal of PI3K signaling, we noticed significant correlation between expression of Entpd5 and these genes (Figure4-3 B-J).

In addition to these co-regulated genes, we also noticed that expression of Forkhead proteins FoxO1 is inversely correlated with expression of Entpd5. This result is consistent with our previous *in vitro* evidence that FoxO family members

suppress Entpd5 transcription while high levels of AKT activation relieve this suppression thus elevating Entpd5 expression.

ENTPD5 expression correlates with AKT activation in human cancer cell lines and primary tumor samples

PTEN mutation and AKT activation are common features for human cancer. As shown in Chapter 2, Entpd5 expression is elevated in prostate cancer cell line LNCaP and C42 which have high AKT activation. We also examined ENTPD5 expression and AKT activation in primary human tumor samples by staining two adjacent sections from a formalin-fixed, paraffin-embedded human primary prostate cancer sample with rabbit monoclonal antibodies against human ENTPD5 and phosphoAKT, respectively. The specificity of this anti-ENTPD5 antibody was verified by western blotting analysis using LNCaP cell lines with or without their ENTPD5 knocked down (Fig.4-4A). The staining intensity for ENTPD5 in tumor was significantly greater compared with adjacent normal tissue and correlated with pAKT staining (Fig.4-4B). Out of 5 samples from patients between ages 57 to 71, only one tumor sample from one 57 years-old patient did not show strong ENTPD5 staining and the same tumor was also negative for pAKT (Fig.4-4B). The remaining four samples showed greater tumor staining of pAKT and ENTPD5 (Fig.4-4B).

Discussion:

Microarray data analysis also indicated that Entpd5 is related to glycosylation and MAPK signaling.

MAPK kinase may regulate Entpd5 through FoxO in a similar way as AKT. Among those genes co-regulated with Entpd5 (Figure 4-5), EGF is a direct activator for RTK signaling and downstream PI3K and ERK signaling cascades. Ras oncogene encodes a small GTPase which directly activate ERK signaling pathway(Nyati et al., 2006). In addition, Cadherin-1 encodes E-Cadherin, which binds to PI3K complex and activates PI3K/AKT signaling(De Santis et al., 2009). MAPKSP1 encodes MAPK scaffold protein 1 which binds to binds to MAP kinase kinase MAP2K1/MEK1, MAP kinase MAPK3/ERK1, and MAP kinase MAPK1/ERK2 and promote cell proliferation (Schaeffer et al., 1998). Zip7 encodes a Zinc transporter located in ER membrane. ZIP7 releases Zinc from endoplasmic reticulum resulting in activation of MAPKs, tyrosine kinase and EGFR(Hogstrand et al., 2009). Expression of these genes is correlated with activation of RTK signaling and PI3K pathway.

Besides RTK signaling components, there are several other genes co-regulated with Entpd5. Many of these regulated genes are involved in glycosylation (GalNac-transferase 7 and Dolichyl-phosphate mannosyltransferase 3, *etc*) and ER stress response (Glutathione reductase and Sec 22, *etc*). This may indicate that these tumors require ENTPD5 and these glycosylation enzyme as well ER stress related protein to deal with high protein influx to ER during rapid protein synthesis.

Materials and Methods:

Luciferase Reporter Assay

The human entpd5 promoter construct (-1000/+1 kb) was cloned from genomic DNA isolated from Hela cells by PCR using the primers, forward: 5'-GGGTACC CATTAAAT TTTGTATGTGTAAG-3' and reverse: 5'-CCTCGAGTGGACAGAAAAAGAATTA-3'. The cloned promoter was then ligated into the pGL3-pro Firefly Luciferase reporter vector (Promega). Transient transfections were carried out after the 293T cells were seeded in Opti-MEM medium using Lipofectamine 2000 (Invitrogen), following the manufacturer's instructions. The pRL-CMV Renilla luciferase reporter vector (Promega) was co-transfected in each experiment and used as an internal control in order to normalize for transfection efficiency. 24 hours later, cells were treated as indicated in the figures. Luminescence was measured using Duo-Glo Luciferase Assay System (Promega) following manufactory instruction.

Gel Shift Assay

Gel shift assay was performed using LightShift Chemiluminescent EMSA Kit (Piercenet, Cat# 20148) according to the manufacturer's recommendations. Following biotin-labeled DNA probes were used: wild type probe, 5'-CCTTGTTTCATTGTTTAG AA-3'; mutant probe 5'-CCTTCCTTCATTGCTGAGAA-3'. Corresponding DNA without biotin label was used as cold competitor.

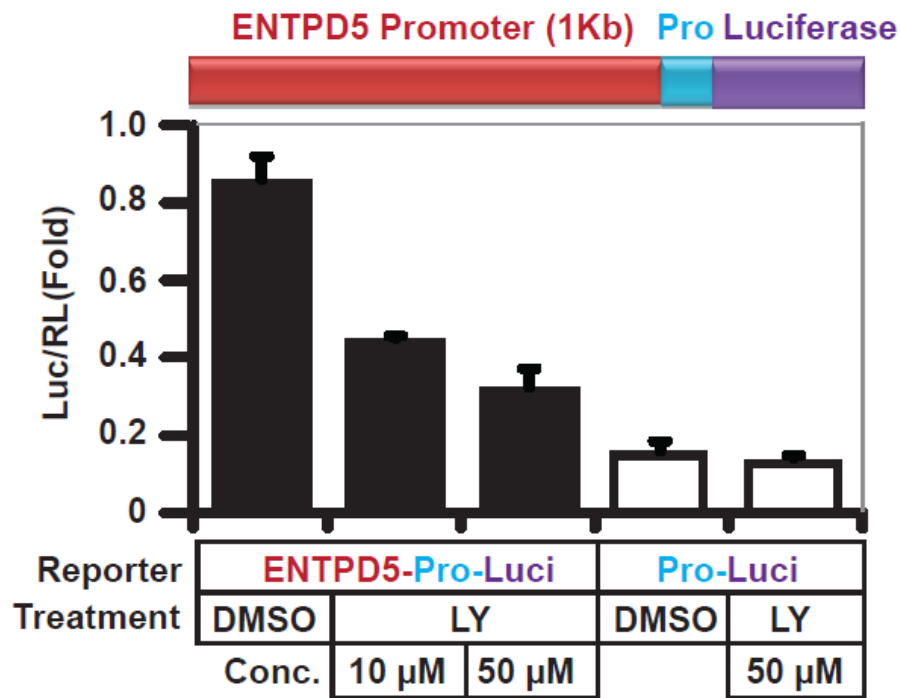
Chromatin Immunoprecipitation (ChIP) Assay

ChIP assay was performed using SimpleChIP™ Enzymatic Chromatin IP Kit (Cell Signaling, Cat# 9002) according to the manufacturer's recommendations. Briefly, prior to harvesting, cells were incubated in 1% formaldehyde solution for 10 min and genomic DNA was extracted, subsequently digested by Micrococcal Nuclease. DNA fragments were immunoprecipitated by different antibodies (anti-Histone H3, Cell Signaling, Cat# 2650; anti-FoxO3, Santa Cruz, Cat# sc-11350). The immuno-precipitated DNA was then analyzed using following primers for ENTPD5 promoter: forward, 5'-CATGTTGCCTAGGCTGGTCTT-3'; reverse, 5'-TTATCTACAAAATCAAACCTT-3'.

Microarray Data analysis

Microarray Dataset is transcription profile of normal, tumor and pure stromal tissue samples from patients with prostate adenocarcinoma (Bermudo et al., 2008). Normalized data (E-MEXP-1331) are downloaded from ArrayExpress. Normalized data were subjected to cluster analysis using Self-Organization Method (SOM) by Cluster Software(Eisen et al., 1998).

A.



B.

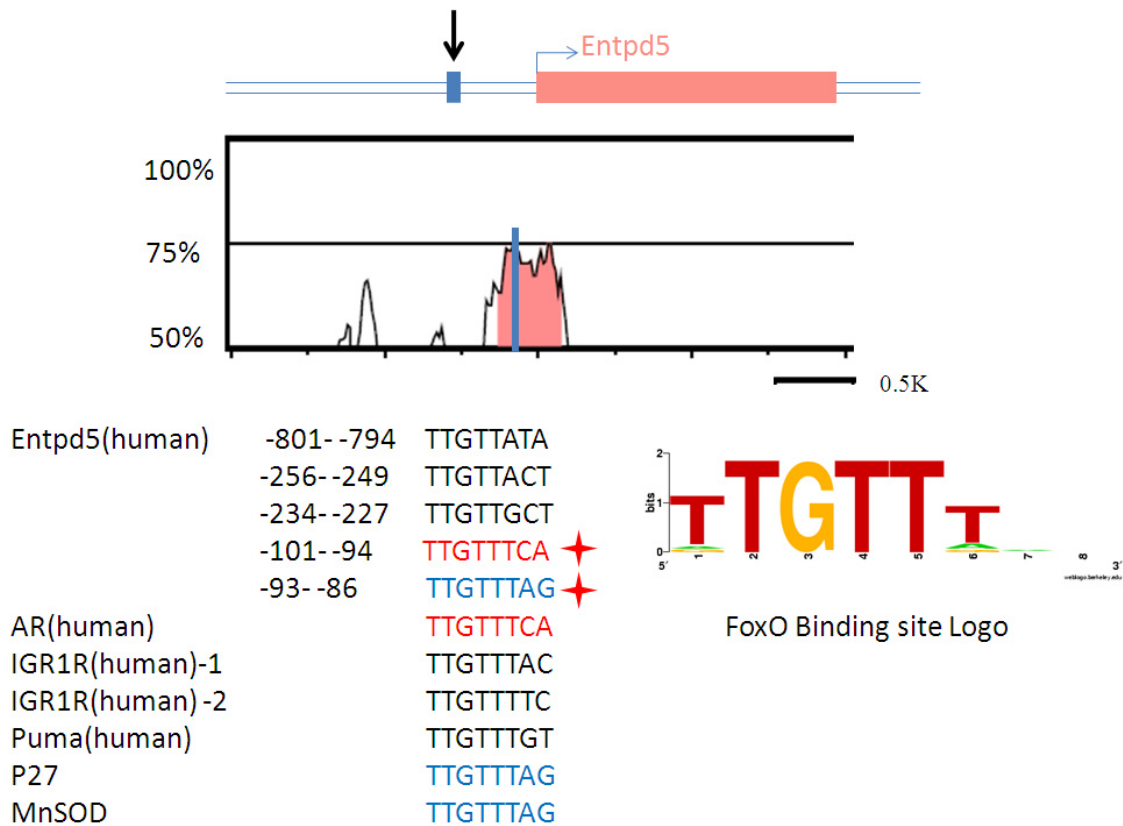
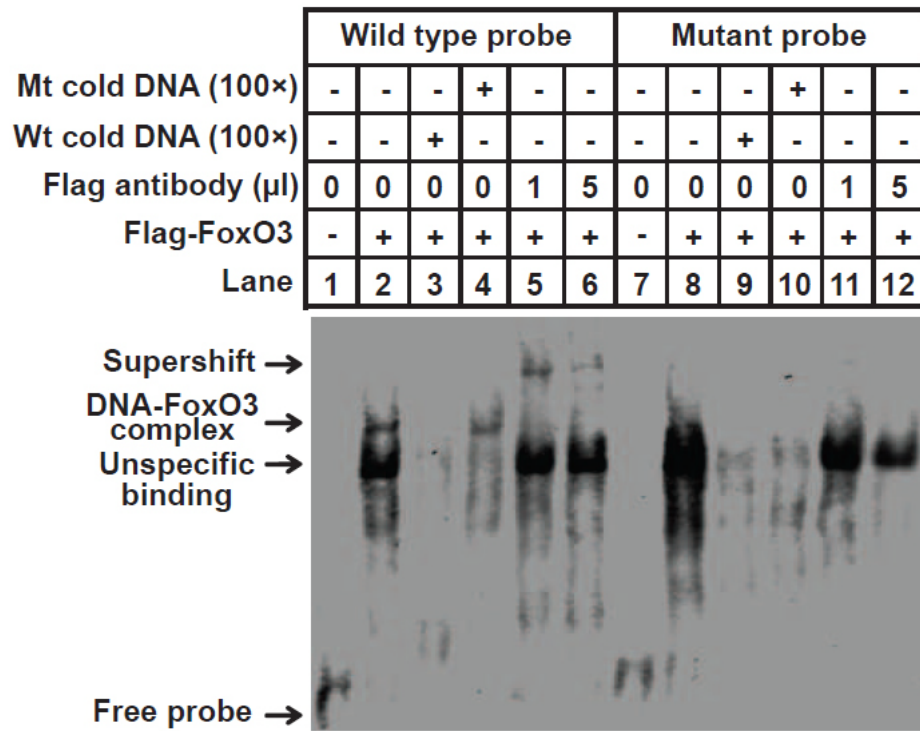


Figure 3-1 Regulation of Entpd5 promoter by PI3K signaling pathway

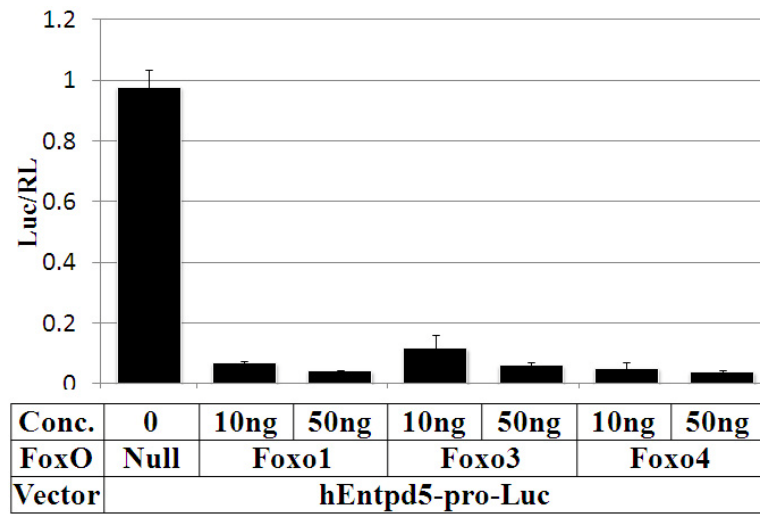
(A)PI3K inhibitor LY294002 represses ENTPD5 promoter activity. Luciferase reporter assay was performed as described in Supplementary Experimental Procedures. Data shown is representative of three independent experiments. Error bars indicate standard deviations.

(B)Identification of conserved FoxO binding sites in the human and mouse Entpd5 promoters. Genomic sequences of human and mouse are aligned according to their similarity. The pink regions have more than 50% similarity. The blue bar indicating the most conserved FoxO binding sites are located in conserved regions. Potential binding sites are similar to known FoxO binding sites as shown in FoxO binding site logo.

A.



B.



C.



Figure 3-2. Regulation of Entpd5 by FoxO family transcription factors.

(A). FoxO3 binds to potential FoxO binding sites in ENTPD5 promoter region.

Lysates containing Flag-FoxO3 protein causes upshift of DNA probe (Lane2 versus Lane 1); mutation of key binding sites abolishes FoxO3 binding (Lane8 versus Lane2, Lane10 versus Lane4); while Flag antibody causes further supershift of DNA probe (Lane5/6 versus Lane 2). See Supplementary Experimental Procedures for detail.

(B).Entpd5 promoter activity is repressed by FoxO family members. co-transfection of FoxO family members (FoxO1-4) with ENTPD5 promoter controlled luciferase reporter represses ENTPD5 promoter activity. Data shown is representative of three independent experiments. Error bars indicate standard deviations.

(C).Chromatin Immunoprecipitation of FoxO3-promoter complexes. Suppression of PI3K signaling pathway induces binding of FoxO3 to ENTPD5 promoter in vivo. Chromatin Immunoprecipitation Assay was performed to visualize binding of FoxO3 to ENTPD5 as described in Supplementary Experimental Procedures. In LNCaP cells, FoxO3 majorly localized in cytosol and did not bind to ENTPD5 promoter. When

LNCaP cells were treated with PI3K inhibitor LY294002, FoxO3 translocated to nucleus and bound to ENTPD5 promoter (Lane7 versus Lane3).

A.

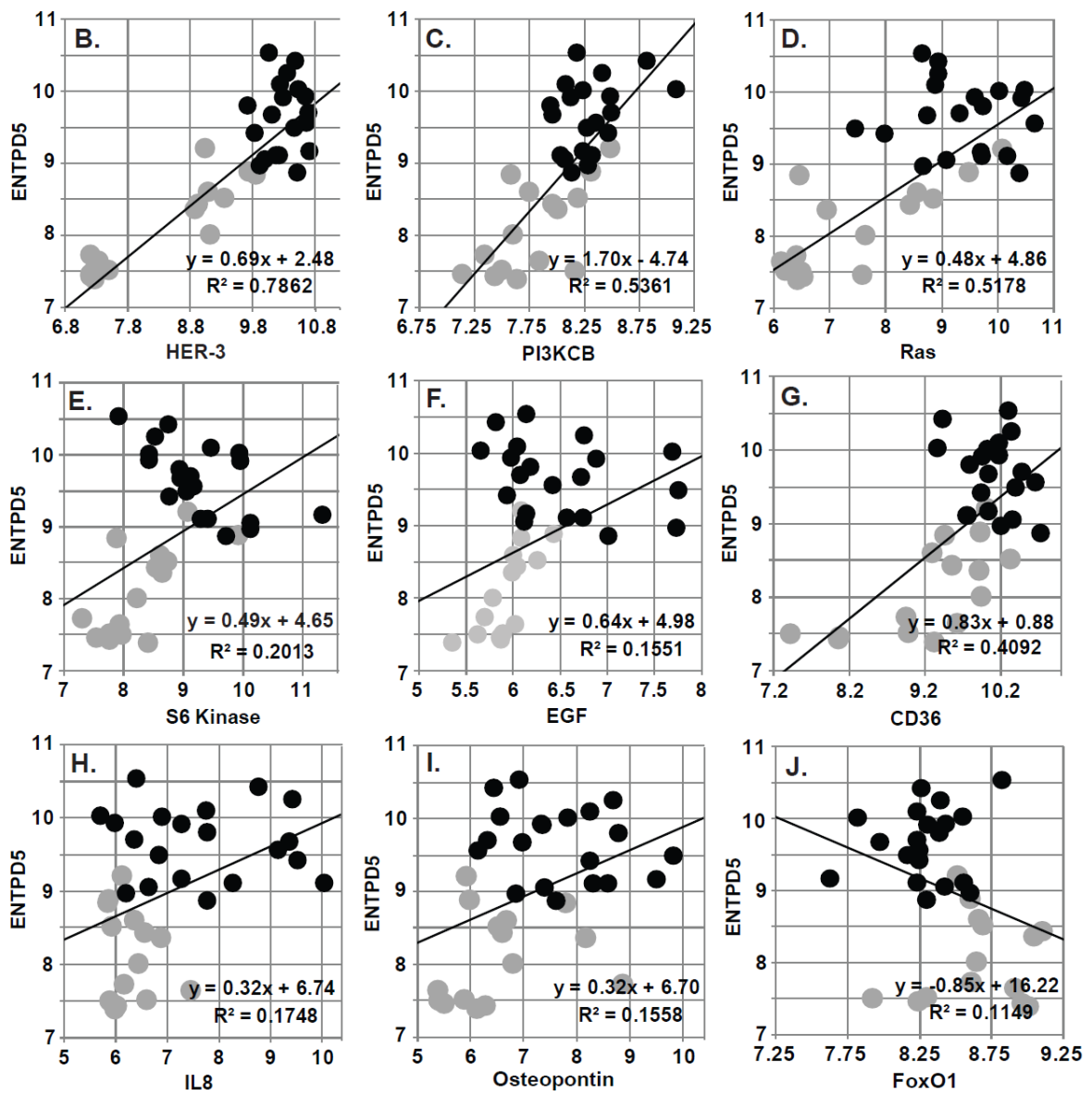
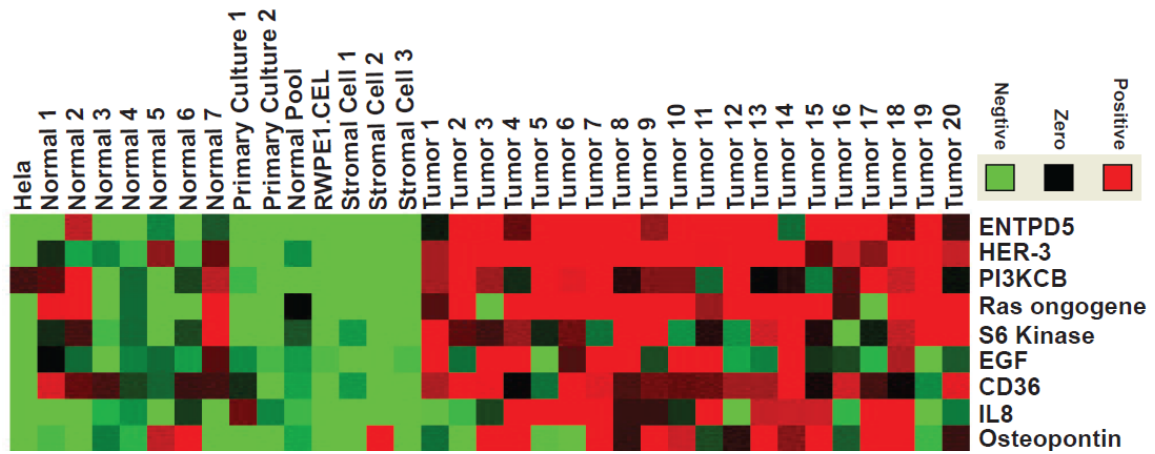


Figure 3-3. Microarray Analysis of Prostate Cancer Tissue Samples

(A) Gene expression profile from prostate tumor microarray data was visualized after cluster analysis with SOM (Self-Organization Method). ENTPD5 is highly expressed in tumor samples (p value=9.15E-10).

(B)-(J) Correlation of ENTPD5 expression with PI3K signaling markers. Normalized ENTPD5 expression level is drawn against HER-3(B); PI3KCB(C); Ras(D); S6 Kinase(E); EGF(F); CD36(G); IL8(H); Osteopontin(I) and FoxO1(J) respectively. R2 (correlation coefficient) is shown in each panel.

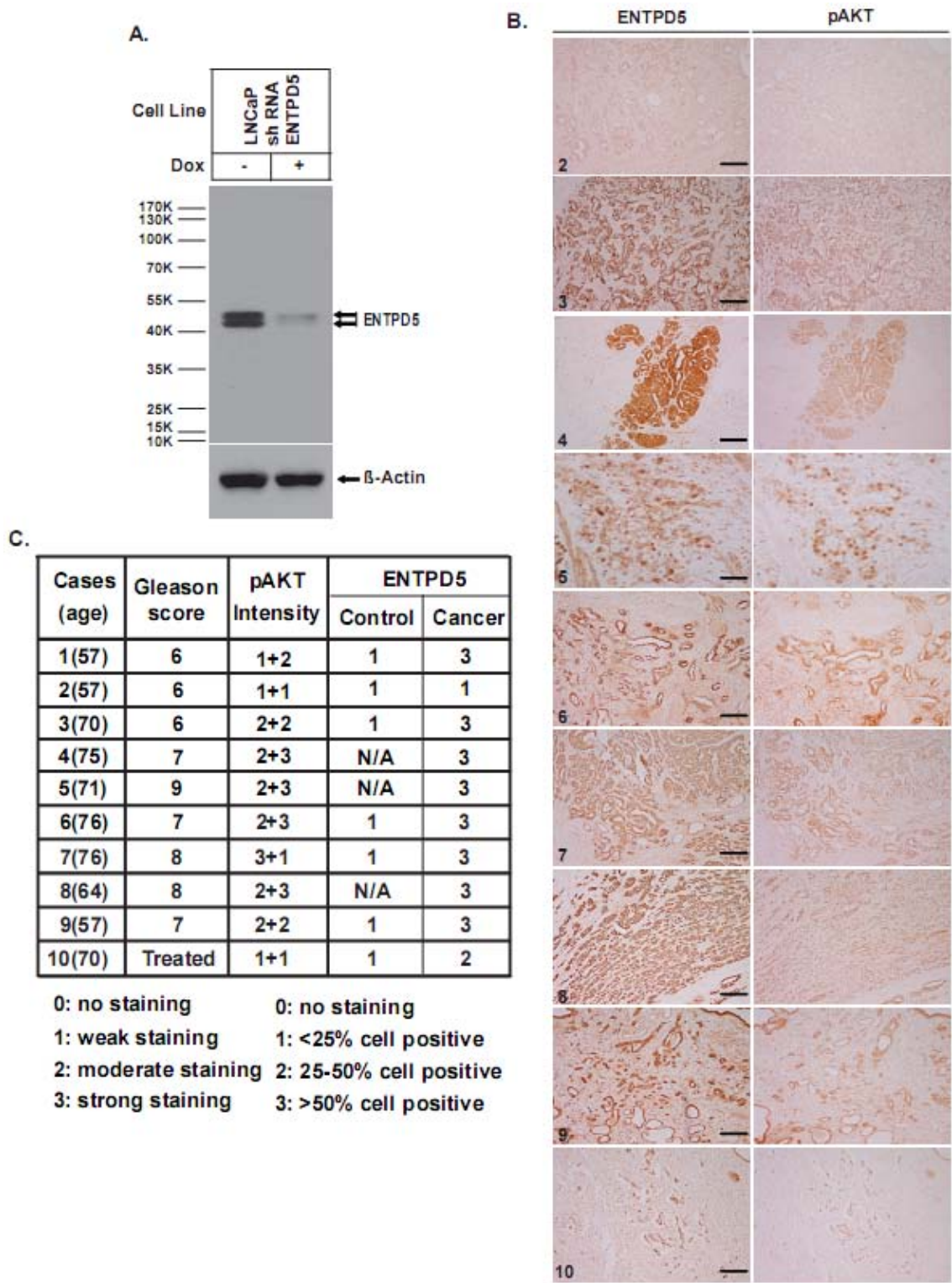


Figure 3-4. Correlation of ENTPD5 Expression with AKT Activation in Human Prostate Cancer Tissue

(A) Total cell lysates as indicated (10 μg) were subjected to SDS PAGE followed by western blot analysis of ENTPD5 (Epitomics, Cat# 2997, 1:15000) and β-Actin.

(B) Immunoperoxidase staining for ENTPD5 (left panel) and pAKT (right panel) in human prostatic carcinoma tissues (patient 2-10). Scale bar for patients 2, 3, 4, 6, 7, 8, 9, 10 (10×), 200μM; scale bar for patient 5 (20×), 100μM.

(C) Summary of status of ENTPD5 expression and AKT activation. See Supplementary Experimental Procedures for detail.

A

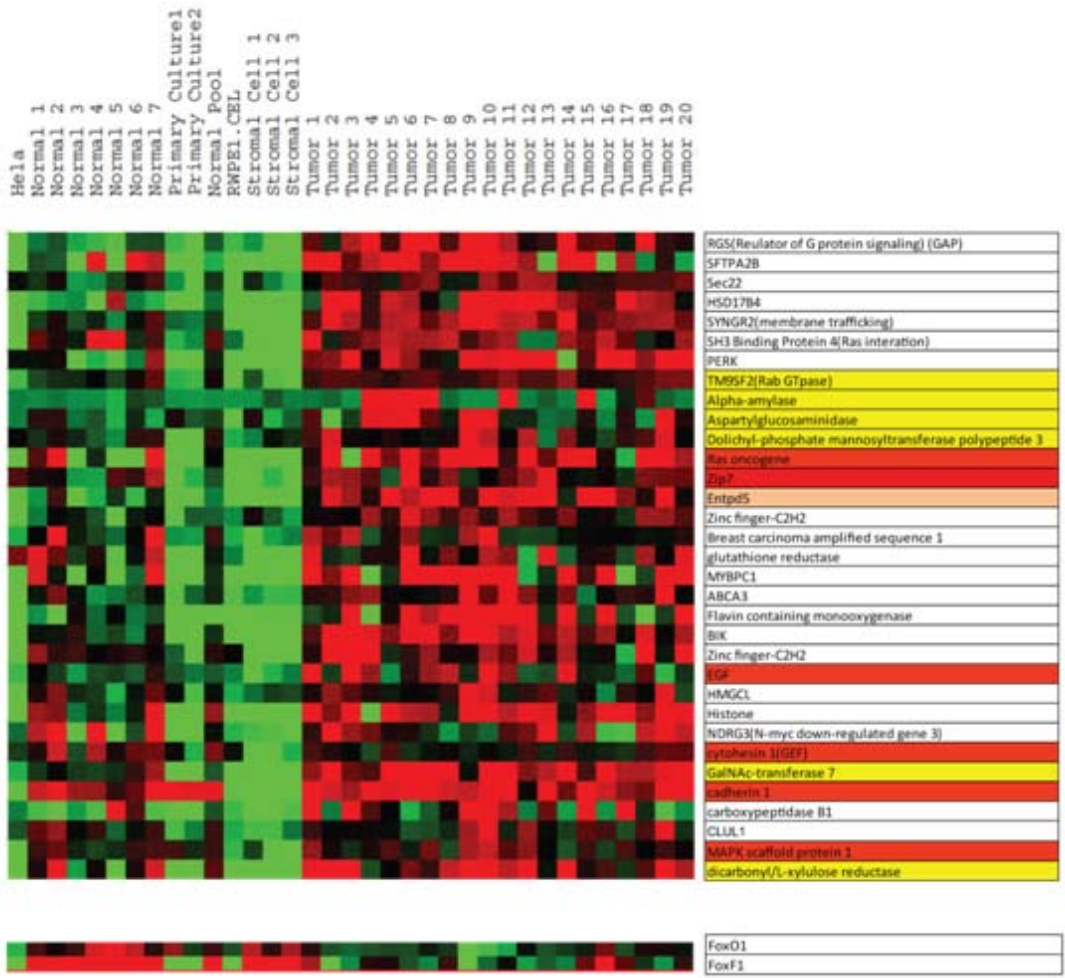


Figure 3-5 Co-Expression of Entpd5 with RTK signaling components and glycosylation related genes.

Microarray data from prostate cancer tissue samples are clustered according to their expression pattern by SOM method. Entpd5 is highly expressed in tumor samples. Some co-expressed genes are involved in activating RTK signaling and downstream PI3K and ERK cascades (Left panel, red filled rows). Some co-expressed genes are involved in regulation of glycosylation (Left panel, yellow filled rows). Expression of FoxO1 transcription factor is reverse correlated with Entpd5 expression.

Reference:

Bermudo, R., Abia, D., Ferrer, B., Nayach, I., Benguria, A., Zaballos, A., del Rey, J., Miro, R., Campo, E., Martinez, A.C., *et al.* (2008). Co-regulation analysis of closely linked genes identifies a highly recurrent gain on chromosome 17q25.3 in prostate cancer. *BMC Cancer* 8, 315.

Biggs, W.H., 3rd, Meisenhelder, J., Hunter, T., Cavenee, W.K., and Arden, K.C. (1999). Protein kinase B/Akt-mediated phosphorylation promotes nuclear exclusion of the winged helix transcription factor FKHR1. *Proc Natl Acad Sci U S A* 96, 7421-7426.

Brunet, A., Bonni, A., Zigmond, M.J., Lin, M.Z., Juo, P., Hu, L.S., Anderson, M.J., Arden, K.C., Blenis, J., and Greenberg, M.E. (1999). Akt promotes cell survival by phosphorylating and inhibiting a Forkhead transcription factor. *Cell* 96, 857-868.

De Santis, G., Miotti, S., Mazzi, M., Canevari, S., and Tomassetti, A. (2009). E-cadherin directly contributes to PI3K/AKT activation by engaging the PI3K-p85 regulatory subunit to adherens junctions of ovarian carcinoma cells. *Oncogene* 28, 1206-1217.

Eisen, M.B., Spellman, P.T., Brown, P.O., and Botstein, D. (1998). Cluster analysis and display of genome-wide expression patterns. *Proceedings of the National Academy of Sciences of the United States of America* 95, 14863-14868.

Fei, M., Zhao, Y., Wang, Y., Lu, M., Cheng, C., Huang, X., Zhang, D., Lu, J., He, S., and Shen, A. (2009). Low expression of Foxo3a is Associated with Poor Prognosis in Ovarian Cancer Patients. *Cancer Investigation* 27, 52-59.

Fernandez de Mattos, S., Essafi, A., Soeiro, I., Pietersen, A.M., Birkenkamp, K.U., Edwards, C.S., Martino, A., Nelson, B.H., Francis, J.M., Jones, M.C., *et al.* (2004). FoxO3a and BCR-ABL Regulate cyclin D2 Transcription through a STAT5/BCL6-Dependent Mechanism. *Mol Cell Biol* 24, 10058-10071.

Hogstrand, C., Kille, P., Nicholson, R.I., and Taylor, K.M. (2009). Zinc transporters and cancer: a potential role for ZIP7 as a hub for tyrosine kinase activation. *15*, 101-111.

Kel, A.E., Gossling, E., Reuter, I., Cheremushkin, E., Kel-Margoulis, O.V., and Wingender, E. (2003). MATCH: A tool for searching transcription factor binding sites in DNA sequences. *Nucleic Acids Res* 31, 3576-3579.

Lam, E.W., Francis, R.E., and Petkovic, M. (2006). FOXO transcription factors: key regulators of cell fate. *Biochem Soc Trans* 34, 722-726.

Lynch, R.L., Konicek, B.W., McNulty, A.M., Hanna, K.R., Lewis, J.E., Neubauer, B.L., and Graff, J.R. (2005). The progression of LNCaP human prostate cancer cells to androgen independence involves decreased FOXO3a expression and reduced p27KIP1 promoter transactivation. *Mol Cancer Res* 3, 163-169.

Nyati, M.K., Morgan, M.A., Feng, F.Y., and Lawrence, T.S. (2006). Integration of EGFR inhibitors with radiochemotherapy. *Nat Rev Cancer* 6, 876-885.

Packer, L., Pavey, S., Parker, A., Stark, M., Johansson, P., Clarke, B., Pollock, P., Ringner, M., and Hayward, N. (2006). Osteopontin is a downstream effector of the PI3-kinase pathway in melanomas that is inversely correlated with functional PTEN. *Carcinogenesis* 27, 1778-1786.

Read, R., Hansen, G., Kramer, J., Finch, R., Li, L., and Vogel, P. (2009). Ectonucleoside Triphosphate Diphosphohydrolase Type 5 (Entpd5)-Deficient Mice Develop Progressive Hepatopathy, Hepatocellular Tumors, and Spermatogenic Arrest. *Veterinary Pathology Online* 46, 491-504.

Schaeffer, H.J., Catling, A.D., Eblen, S.T., Collier, L.S., Krauss, A., and Weber, M.J. (1998). MP1: a MEK binding partner that enhances enzymatic activation of the MAP kinase cascade. *Science* 281, 1668-1671.

Shiota, M., Yokomizo, A., Kashiwagi, E., Tada, Y., Inokuchi, J., Tatsugami, K., Kuroiwa, K., Uchiumi, T., Seki, N., and Naito, S. (2010). Foxo3a expression and acetylation regulate cancer cell growth and sensitivity to cisplatin. *Cancer Science* 101, 1177-1185.

Tong, K.-M., Shieh, D.-C., Chen, C.-P., Tzeng, C.-Y., Wang, S.-P., Huang, K.-C., Chiu, Y.-C., Fong, Y.-C., and Tang, C.-H. (2008). Leptin induces IL-8 expression via leptin receptor, IRS-1, PI3K, Akt cascade and promotion of NF-[kappa]B/p300 binding in human synovial fibroblasts. *Cellular Signalling* 20, 1478-1488.

van Oort, M.M., van Doorn, J.M., Bonen, A., Glatz, J.F., van der Horst, D.J., Rodenburg, K.W., and Luiken, J.J. (2008). Insulin-induced translocation of CD36 to the plasma membrane is reversible and shows similarity to that of GLUT4. *Biochim Biophys Acta* 1781, 61-71.

Zou, Y., Tsai, W.-B., Cheng, C.-J., Hsu, C., Chung, Y., Li, P.-C., Lin, S.-H., and Hu, M. (2008). Forkhead box transcription factor FOXO3a suppresses estrogen-dependent breast cancer cell proliferation and tumorigenesis. *Breast Cancer Research* 10, R21.

Chapter 4: *In vivo* function of Entpd5

Abstract

Entpd5 is highly expressed in several PTEN null cancer cell lines. Knockdown of ENTPD5 in PTEN null Prostate cancer cell LNCaP induces ER stress and degradation of several receptor tyrosine kinases such EGFR and Her-2. Consequently, Knocking-down ENTPD5 induces apoptosis under protein-overloading conditions and tumor shrinkage in mouse xenograft tumor models.

The degradation of those tyrosine kinase receptors are proteasome dependent and probably through ER-associated degradation pathway. Evidently, knocking-down Entpd5 increased binding of EGFR to ER chaperons such as BiP, Calnexin and Calreticulin.

All these results suggest that Entpd5 is an important component of ER protein quality control system and could be a potential target for anti-cancer therapy.

Introduction

ER is the site for producing proteins destined for ER, Golgi, plasma membrane and secretion. Most of these proteins are glycosylated, either N-linked or O-linked. Nascent peptide chain enters ER lumen in a co-translational manner through Sec61 translocon complex, and at the same time,

Luminal oligosaccharyltransferase(OST) start to transfer a pre-assembled core glycan(as shown in Figure4-1B) to asparagines in consensus Asn-x-Ser/Thr motif in

the peptide from a lipid pyrophosphate donor, dolicol-PP. Then these glycosylated peptides enter a re-glycosylation/de-glycosylation cycle (Figure 4-1A) which helps them folding by glycoprotein specific chaperon systems. This chaperon system contains calnexin and calreticulin which binds only to mono-glycosylated proteins (As shown in Figure 4-1C). Therefore, two glucoses on branch A in N-glycan of co-translated peptide need to be removed sequentially by two glycanases glucosidase I (GI) and glucosidase II (GII) so they can bind to calnexin/calreticulin. Subsequently, the third glucose is removed by GII so the protein can be further processed according to its folding status; they can either (1) exit to Golgi for further processing if they fold correctly, or (2) retrotranslocate to cytosol and be degraded by ER-Associated Degradation (ERAD) system if they are terminally misfolded, or (3) be reglycosylated by UDP-Glucose:Glycoprotein glycotransferase(UGGT) (Molinari, 2007). Reglycosylation allows incomplete folded glycoprotein re-enters association with calnexin/calreticulin. The removal and addition of glucose allows the binding and release of calnexin/calreticulin until the proteins are correctly folded and transferred to Golgi. However, UDP will be generated as a by-product in reglycosylation step and inhibits UGGT activity and, therefore slows down the reglycosylation/deglycosylation cycle.

Presumably inhibition of UGGT by UDP will lead to defective protein folding, especially under stress conditions. As shown in previous chapter, ENTPD5 is an UDPase located in ER. It may function by converting UDP to UMP relieving

inhibition of UGGT and thus providing antiporter metabolite UMP for UDP-Glucose entrance into ER lumen.

Results and Discussions

Knockdown of Entpd5 causes cell death under protein-overload condition

To verify the functional significance of ENTPD5 expression in human cancer cells, we generated LNCaP derived stable cell line in which an shRNA against human ENTPD5 could be induced by Dox. In normal culture condition, knockdown ENTPD5 does not have any significant effect on cell growth or cell survival. This is consistent with previous reports that UGGT null MEF (mouse embryonic fibroblasts) grow and propagate well and does not exhibit any significant morphological change (Molinari et al., 2005) since we hypothesized that ENTPD5 regulates UGGT function by hydrolyzing UDP to UMP in the ER lumen.

We hypothesized that knockdown of ENTPD5 may sensitize cells to ER stress under stress conditions. To test our hypothesis, we used puromycin to induce protein over-loading to increase stress to ER lumen. Puromycin dissociates nascent polypeptide from the ribosome and the translocon, and increases ER loading of unfolded proteins (Blobel and Sabatini, 1971; Oyadomari et al., 2006). Inducing ENTPD5 knockdown by adding Dox caused significant cell death when these ENTPD5 knocking-down LNCaP cells were treated with puromycin for 24 hours (Figure4-2A, column 6, 7 and 8). This type of cell death is apoptosis as caspase 3 activity significantly increased after treating Entpd5 knocking-down cells with puromycin (Figure4-2B). To confirm the

above-mentioned apoptosis phenotype after ENTPD5-targeting shRNA expression was specific, we introduced into these cells a cDNA encoding ENTPD5 with silent mutations in the shRNA target sequence. In these cells, although the endogenous ENTPD5 was still knocked down after addition of Dox (Figure4-3C, lanes 2 and 6), the expression of an shRNA resistant wild type transgene (three flag tags were fused to ENTPD5 coding sequence so it migrated higher) led to reversal of upregulation of Caspase 3 activity(Figure4-2C). In contrast, introducing an E171A mutant (Entpd5 CD) that abolishes UDP hydrolysis activity of ENTPD5 was not able to decrease Caspase 3 activity.

Knockdown of Entpd5 causes ER stress under protein-overload conditions

To further elucidate the mechanism about how knocking down Entpd5 induced cell death, we examined the expression of components from ER stress signaling and cell death pathway. Interesting, we found that knockdown of Entpd5 induces ER stress as shown by unregulated expression of ER chaperon BiP and CHOP under protein-overloading condition by treating cells with puromycin (Figure4-3A, Lane 8 and Lane 12). In addition, under protein-overloading conditions, knocking down Entpd5 also leads to decreased expression of receptor tyrosine kinase such as EGFR and Her-2, and at mean time leads to cleavage of Caspase 3, the primary executioner Caspase which correlated with upregulation of Caspase 3 activity. Another marker of ER stress, spliced Xbp1 is also induced by knocking down Entpd5. On activation of ER stress, activated IRE1 endonuclease removed 26nt from unspliced form of Xbp1

mRNA(473bp by RT-PCR) and generated a spliced short form of mRNA(447bp by RT-PCR).

Expression of receptor tyrosine kinase was restored to the normal level by expression of shRNA-resistant wild type ENTPD5 transgene (Figure4-3C, lanes 5-6) but not the active site mutant (Figure4-3C, lanes 7-8). The induction of BiP and cleavage of Caspase 3 are also suppressed by wild type ENTPD5 transgene but not catalytic dead mutant (Entpd5 CD) (Figure4-3C).

EGFR is degraded in ER-associated degradation pathway

We hypothesized that tyrosine kinase receptors are degraded by ER-associated degradation pathway since inducing protein overloading by adding puromycin rapidly led to decrease of EGFR protein and induction of ER stress. This rapid decrease can be blocked by treating cells with proteasome inhibitor MG-132. At the same time, the mRNA level of EGFR did not decrease as shown by RT-PCR. mRNA of Her-2 was slightly decreased. It is possible that ER stress-induced inhibition of transcription and translation also contributed to the decrease of these tyrosine kinase receptors.

It is known that monoglucosylated proteins are retained in the ER by interacting with CNX or CRT. To examine whether EGFR interacts with these chaperons, we performed a co-Immunoprecipitation experiment with extracts from different cells (with or without knocking down Entpd5) using EGFR antibody. Increased presence of CRT and CNX was shown when Entpd5 was knocked down (Figure4-5, lane 6 and 5) or cells were treated with puromycin (Figure4-5, lane 7 and 5). The presence of these

chaperons was also increased when knocked cells are treated with puromycin (Figure4-5, 8 and 5).

We also tested if BiP, another ER chaperon involved in retention of unfolded EGFR. As shown in Figure4-5, co-immunoprecipitated BiP was also increased when Entpd5 was knocked down or cells were treated with puromycin.

Taken together, these results demonstrate that aberrantly glycosylated EGFR is unfolded, retained in ER by CNX/CRT and then degraded by ERAD. We thus concluded that Entpd5 is crucial for ER quality control system of glycosylated proteins.

Knockdown of Entpd5 causes tumor shrinkage in xenograft model

Since AKT activated tumors usually grow very fast *in vivo*, these tumors may encounter ER stress conditions such as hypoxia and cytokine attack. To test whether knocking down ENTPD5 in LNCaP cells also have an effect on their growth *in vivo*, we planted matrix gel-filled LNCaP cells bearing a Dox-inducible shRNA targeting ENTPD5 in nude mice. As a control, LNCaP cells with a Dox-inducible shRNA targeting GFP were also planted. After the xenograft tumors reached the size of 300 mm, 7 mice were fed with Dox-containing water. The level of ENTPD5 in these tumors was measured after 3 weeks. Compared with mice fed with normal water, ENTPD5 levels in tumors from mice fed with Dox-containing water were significantly down except in one mouse (Figure4-6A). While ENTPD5-targeting shRNA containing tumors in mice fed with normal water continued to grow, these tumors in mice feed with Dox-containing water shrank (Figure4-6 B and C). Amazingly, when

these tumor samples were analyzed under a microscope after fixing and staining with hematoxylin and eosin, there was little tumor cell left in the matrix gel in tumors grown in Dox-fed mice while in mice fed with normal water, matrix gels were filled with tumor cells (Figure4-6D). The GFP shRNA-containing tumors did not respond to Dox treatment and continued to grow during the period of experiment.

Discussion:

ENTPD5 is potentially a novel drug target for prostate cancer

The current study highlighted ENTPD5 as a critical link in PI3K/PTEN pathway that promotes cell growth and survival, a pathway that is often activated in cancer cells. Here we showed a nice correlation between ENTPD5 expression and AKT activation in both cultured prostate cancer cell lines and primary human prostate carcinoma samples. Therefore, inhibition of this enzyme, similar to knockdown, can potentially generate benefits for anti-cancer activity. It would induce more severe ER stress in cancer cells with active AKT due to higher protein traffic through the secretory pathway. It may also cause synthetic lethality in these cells, which otherwise maintain survival advantage and resistance to common anti-cancer drugs. Chronic Inhibition of ENTPD5 may cause liver and male fertility defects since mice with ENTPD5 deficiency show hepatopathy and aspermia(Read et al., 2009). These defects in mice, however, only become obvious after 1 year of age. Given the widespread occurrence of PI3K/PTEN mutations in human cancers and potential synthetic lethal effect of AKT activation and ENTPD5 inhibition, to develop ENTPD5 inhibitors for cancer therapy may be a worthwhile pursuit.

Phylogenetic study of UDP hydrolyzing enzyme indicated functional redundancy

ENTPD5 belongs to a family of ER/Golgi localized UDP hydrolyzing enzyme. From literature there are 9 characterized UDP hydrolyzing enzymes from *S.cerevisiae*, *C.elegan* and *H.Sapien*. According to their sequence similarity, these proteins can be divided into 3 classes. Class I (S.Gda1, C.Uda1 and H.Entpd5) and Class II (S.Ynd1, C.Mig-23, C.Ntp1 and H.Entpd4) are conserved from *S.cerevisiae* to *H.Sapien*, while Class III (C.Apy1 and H.Cant1) do not have homolog genes in yeast (Figure4-7A).

Among these genes, several have been shown to regulate ER stress response or glycosylation, S.Gda1 (Class I) (Abeijon et al., 1993), S.Ynd1 and C.Mig-23 (Class II) (Gao et al., 1999; Nishiwaki et al., 2004), and C.Apy1 (Class III) (Uccelletti et al., 2008). In *H.Sapien*, There are 8 Entpd family members. Entpd6 shares better similarity with Entpd5 and can be categorized into Class I; Entpd7 shares similarity with Entpd4 and can be categorized into Class II. It is possible that all these paralog genes such as Cant1, Entpd4, Entpd5, Entpd6 and Entpd7 may have redundant function in ER or Golgi in human (Figure4-7B).

Other Entpd members (Entpd1, Entpd2, Entpd3, Entpd8) are clustered into another class and have been shown to be out-membrane proteins or secreted proteins (Figure4-7C). They may have distinct functions in regulating nucleotide level out of cells.

Materials and Methods:

Antibodies Used

ENTPD5 (Sigma, Cat# HPA002927), PTEN, AKT, phosphorylated AKT, EGF receptor, Her-2/ErbB-2, IGF receptor β subunit, Bip and β -Actin (Cell Signaling, Cat# 9559, 9272, 9271, 2646, 2165, 3027, 3177 and 4970 respectively). Antibody for Tet repressor is from Gene Tex Inc (Cat# GTX70489).

Immunoprecipitation

Cells were lysed with FLAG lysis buffer (50 mM Tris pH 7.4, 150 mM NaCl, 1% Triton supplemented with 1X protease inhibitor cocktail (Roche)). Lysates were cleared by centrifugation at 5000g for 5 minutes. The supernatant was incubated with anti-EGFR-antibody coupled agarose (sc-03 AC from Santa Cruz) overnight at 4 degree. The resulting immunoprecipitates were washed 3 times with the extraction buffer, separated on a 8% SDS-PAGE gel, and analyzed by western blotting using anti-EGFR(#2232 from Cell signaling or #sc-03 from Santa Cruz), anti-CRT(#2891 from Cell signaling or # from), anti-CNX(#2433 from Cell signaling), anti-BiP(from Cell signaling) or anti-ubiquitin(from) antibody.

Cell Culture

Human prostate cancer cell line LNCaP, human colon cancer cell line HT-29, human breast cancer cell line MCF-7, MBA231, SKBR-3 and T47D and attached Hela cell are from ATCC. Other human prostate cancer line PC-3, DU145, LAPC4, and C42 were kindly provided by Dr. Jer-Tsong Hsieh at UT Southwestern. All the

cell lines except LNCaP, T47D and LAPC4 are grown in DMEM medium supplemented with 10% fetal bovine serum (FBS) (Invitrogen) plus 200 unit/ml penicillin/streptomycin (Hyclone). LNCaP and T47D are cultured in RPMI 1640 medium containing 10% FBS plus 200 unit/ml penicillin/streptomycin and 20 mM Glutamine (Hyclone) while LAPC4 is cultured in Iscove's medium supplemented with 10% FBS and 200 unit/ml penicillin/streptomycin.

Cell Survival Assay

Cell survival analysis was performed using the Cell Titer-Glo Luminescent Cell Viability Assay kit (Promega) following manufactory instruction with minor modification. In brief, 25 μ l of Cell Titer-glo reagent was added to the cell culture medium. Cells were place on a shaker for 10 min and were then incubated at room temperature for an additional 10 min. Luminescent reading was carried on Tecan SPECTRAFluor Plus reader (Tecan).

Plasmids and siRNA Oligoes

Entpd5 Expression Constructs

Human Entpd5 (hEntpd5) was cloned into modified pCI-Neo vector with C-terminal 3xFlag tag.

Entpd5 shRNA constructs:

Six tandem hEntpd5 shRNA (5'-CAT ATT AGC TTG GGT TAC T-3') expression cassettes driven by H1 promoter were cloned into pSuperior.puro vector following the

protocol as previously described.

Rescue experiment constructs:

The shRNA resistant hEntpd5 (sr-hEntpd5) expression construct was generated by introducing four silent point mutations within the shRNA targeted region (5'-CAT CTT AGC CTG GGT CAC C-3') of pCI-Neo-hEntpd5-3xFlag.

For the catalytic-dead form of human Entpd5 (sr-hEntpd5CD), hEntpd5 E172A mutation was introduced by site directed mutagenesis in the above shRNA resistant expression construct.

RT-PCR

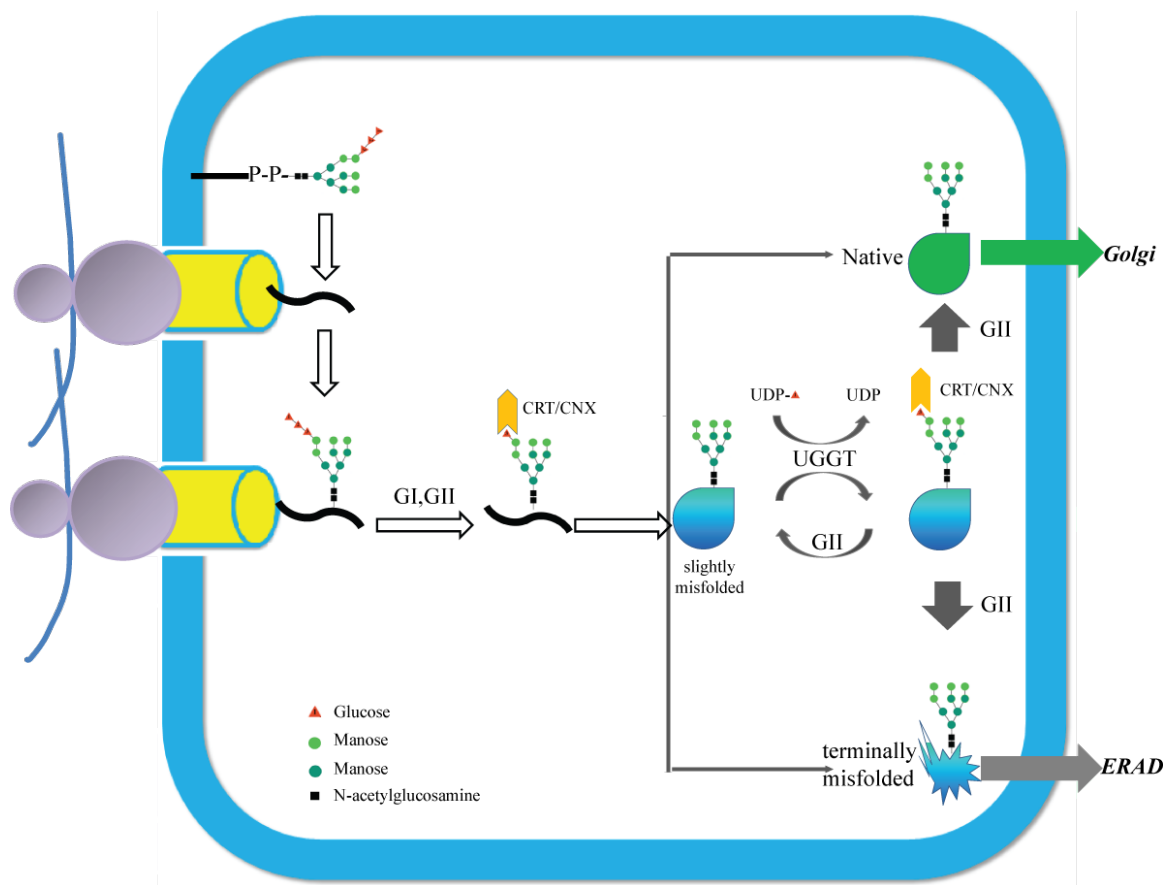
LNCaP-shRNA-GFP and LNCaP-shRNA-ENTPD5 cell lines were cultured as described in Methods. After adding Dox for 6 days, total RNA from each cell lines was extracted by the Trizol reagent (*Invitrogen*). One microgram of total RNA was used for first strand cDNA synthesis with superscript reverse transcriptase (RT) (*Invitrogen*). RT-PCR was performed using following primers for each gene.

Gene	RT PCR primers	Amplicon Size
EGFR	5'-TCTCAGCAACATGTCGATGG-3'	475bp
	5'-TCGCACTTCTTACACTTGCG-3'	
Her-2	5'-CTGAACTGGTGTATGCAGATTGC-3'	82bp
	5'-TTCCGAGCG GCCAAGTC-3'	
IGFR	5'-TGGGGAATGGAGTGCTGTAT-3'	450bp
	5'-CGGCCATCTGAATCATCTTG-3'	
ENTPD5	5'-CTTTCCGGAGTGCCTGTTTA-3'	434bp
	5'-AGCCCGTCTCTATGTTGTTCACTT-3'	
β -Actin	5'-GTGGGGCGCCCCAGGCACCA-3'	539bp
	5'-CTCCTTAATGTCACGCACGATTTC-3'	

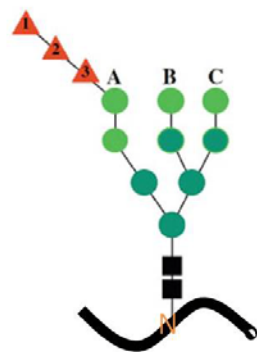
Xenograft Studies

LNCaP stable cell lines (2×10^6) in 100 μ l of Matrigel were inoculated into the flank of 8-week-old male nude mice. After 2 weeks, tumors reached 0.5-1 cm^3 . Mice were distributed randomly into two groups (around 7 animals each) for the subsequent analysis of tumor development with and without Dox-treatment. Dox (Sigma) was applied as 2 mg/ml solution via the drinking water with additional 1% sucrose dissolved in natural mineral water starting 2 weeks after inoculation. Drinking water for control mice contained 1% sucrose without Dox. Xenografted tumors were measured by a sliding caliper once a week. Absolute tumor volumes were evaluated according to $\text{Volume} = (\text{width})^2 \times \text{length}/2$. Relative tumor volumes represent the ratio of current tumor volume and corresponding volume at the beginning of the study. After inoculation measurements started at week 3 and finished at week 8 followed immediately by sacrificing the animals. Eight individual tumors from the Dox-treated as well as from the untreated groups were analyzed. Tumor protein was extracted and subjected to western blotting. Tumor samples were harvest, fixed and stained with hematoxylin and eosin, and examined with a digital camera.

A.

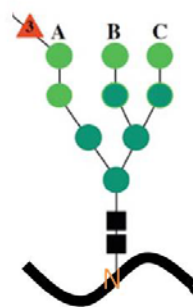


B.



pre-assembled polypeptide

C.



monoglucosylated polypeptide

Figure4-1. Reglucosylation cycle of glycoprotein in Endoplasmic Reticulum.

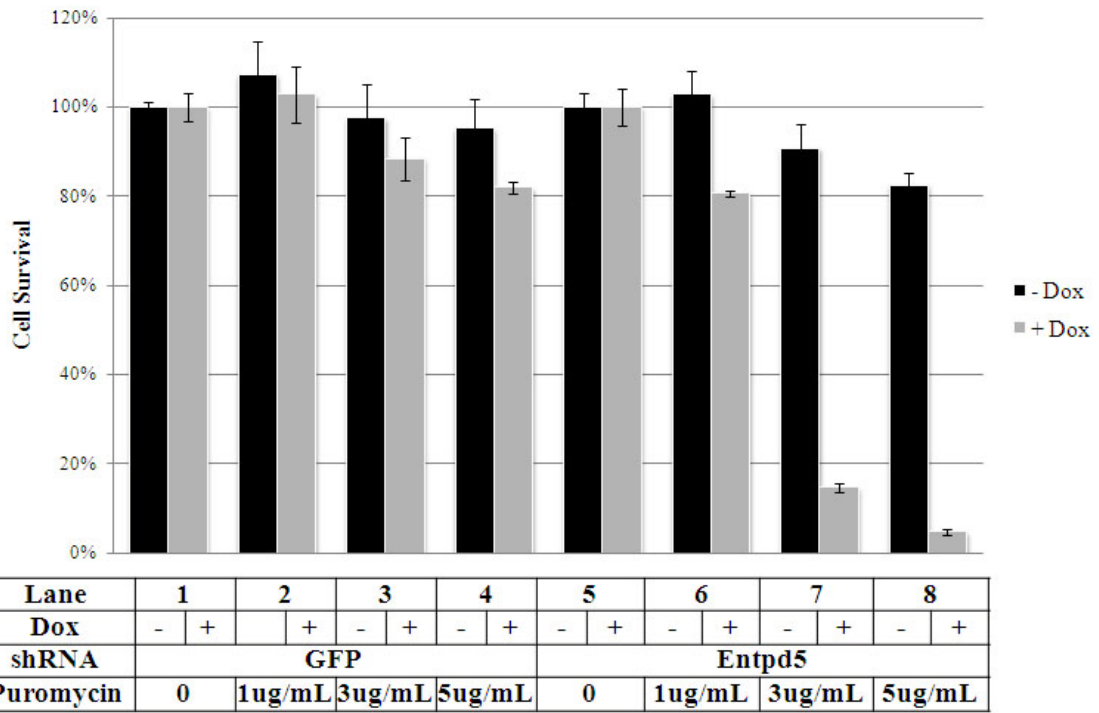
(A). After addition of the pre-assembled oligosaccharide the two outermost glucoses (red triangle) are removed and the nascent polypeptide associates with

calnexin/calreticulin (CRT/CNX). Most glycopolypeptides are probably released as native proteins and exit the ER. Misfolded proteins are then reglucosylated and enter cycles of dissociation/re-association with CRT/CNX. The correctly folded proteins then exit ER, while terminally misfolded proteins are degraded through ER-Associated degradation pathway (Modified from (Ruddock and Molinari, 2006))

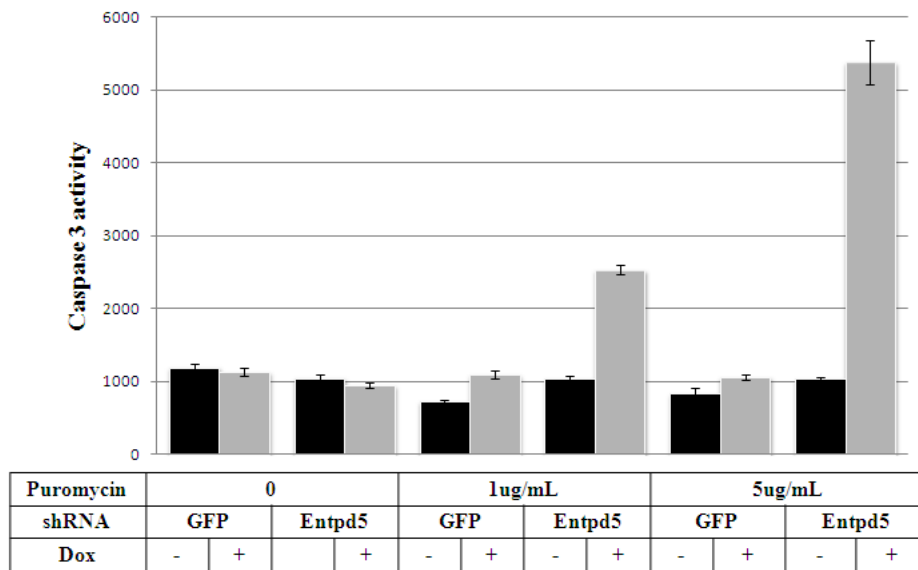
(B). polypeptide with pre-assembled oligosaccharide

(C). monoglucosylated polypeptide

A.



B.



C.

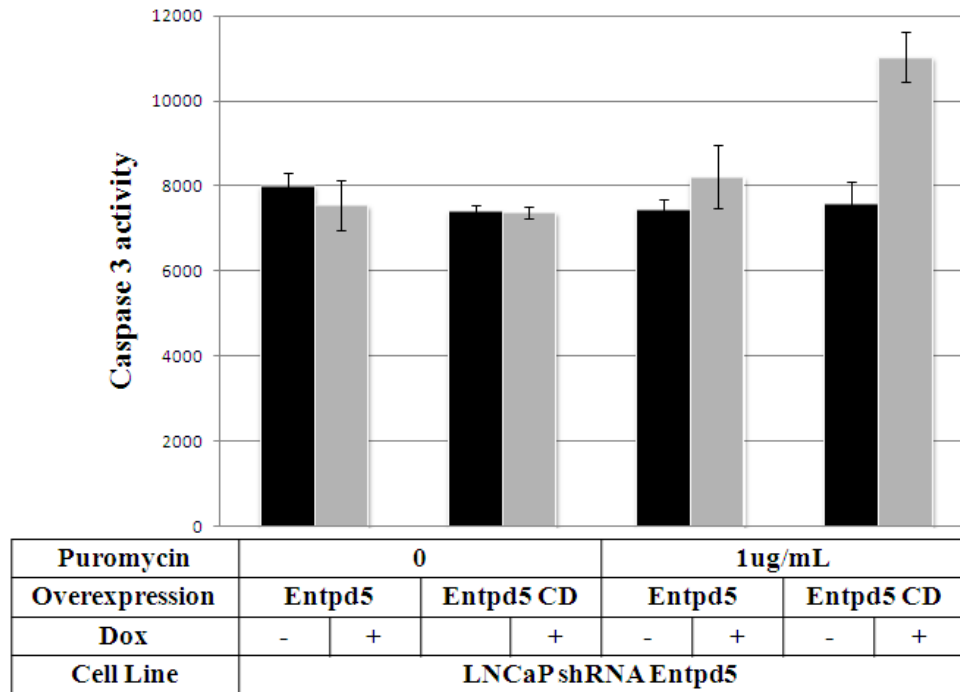


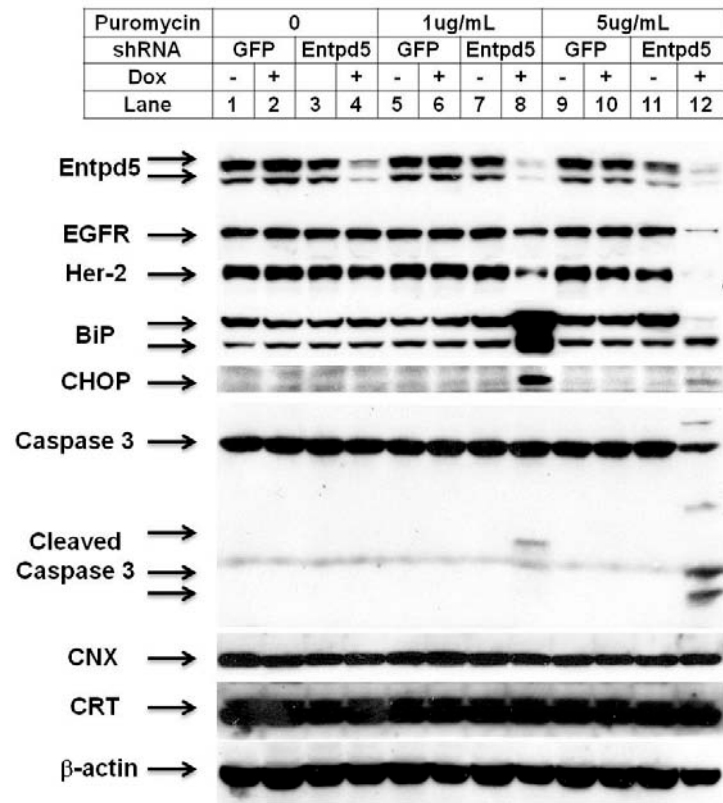
Figure4-2 Knockdown ENTPD5 causes cell death under protein-overload conditions

(A).Knocking-down Entpd5 sensitized LNCaP cells to puromycin-induced protein overloading at dosage dependent manner. After knocking Entpd5 by adding dox for 3 days, puromycin at indicated concentrations were added to induce protein overloading. Cell viability were measured by Cell-titer glo as in Materials and Methods.

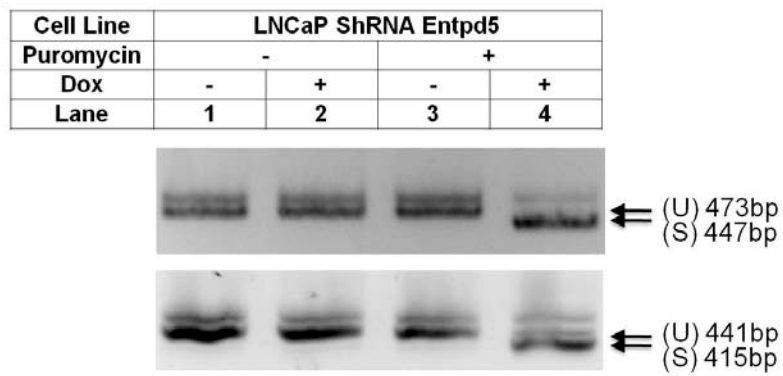
(B).Caspase 3 activity increased after inducing protein overloading in Entpd5 knocking-down LNCaP cells but not in GFP knocking-down control cells. Caspase 3 activity was measured using fluorogenic substrate as in Materials and Methods.

(C).Ectopic-expression of Entpd5 but not the catalytic dead form of Entpd5 (Entpd5 CD) reversed upregulation of Caspase 3 activity.

A.



B.



C.

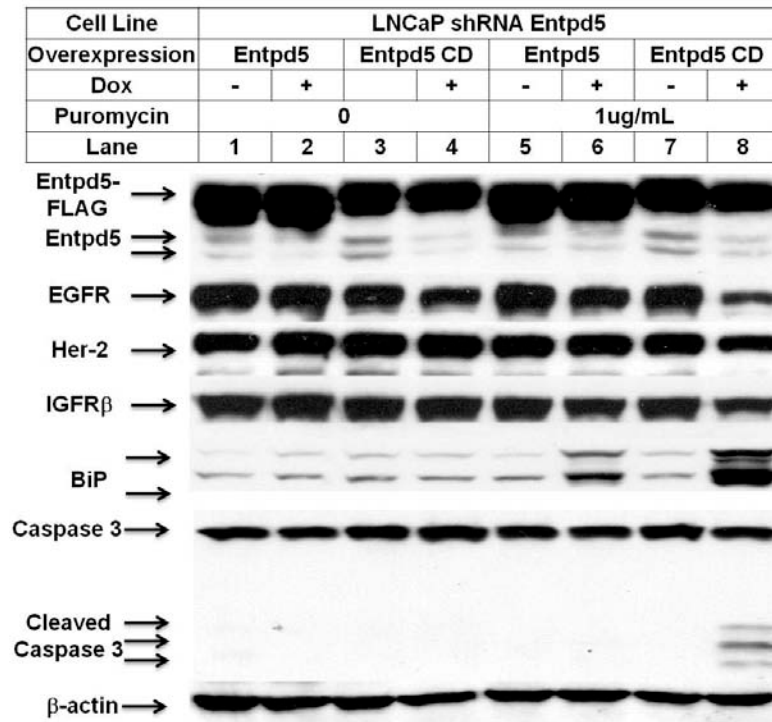


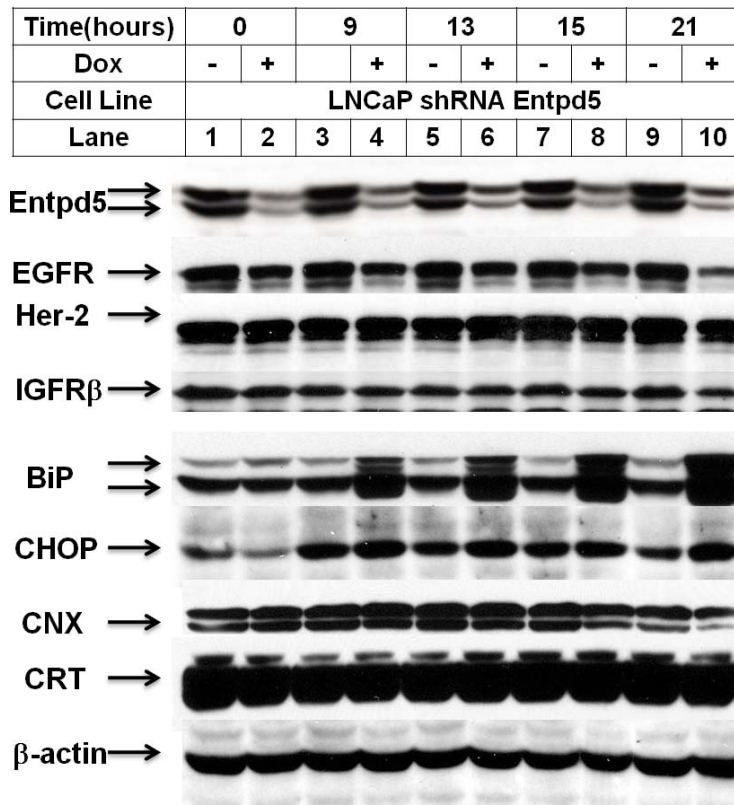
Figure4-3 Knocking-down Entpd5 induced ER during protein-overloading condition.

(A).Knocking-down Entpd5 induced BiP and CHOP up-regulation under protein-overloading conditions induced by puromycin. Entpd5 was knockdown by adding doxycycline. Protein overloading was induced by puromycin. Cell lysates were separated by SDS-PAGE and blotted with antibodies as indicated. Tyrosine kinase receptors (EGFR and HER2) decreased and Caspase 3 was cleaved after knocking down Entpd5.

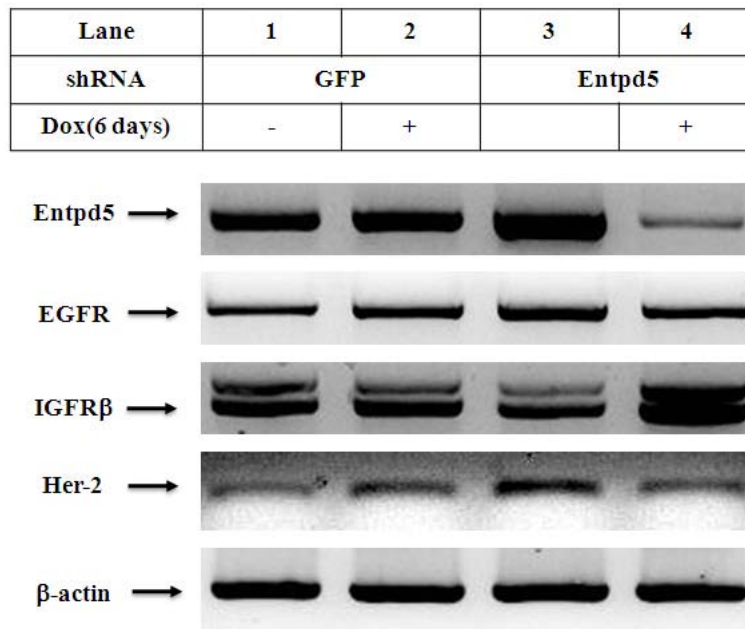
(B).Knocking-down Entpd5 induced xbp1 splicing under protein-overloading conditions induced by puromycin. (U) is 473bp RT-PCR product from unspliced Xbp1 mRNA; (S) is 447bp RT-PCR product from spliced Xbp1 mRNA.

(C).Overexpression an shRNA-resistant Entpd5 but not the catalytic dead form of Entpd5 (Entpd5 CD) attenuated BiP upregulation and reversed Caspase 3 activation.

A.



B.



C.

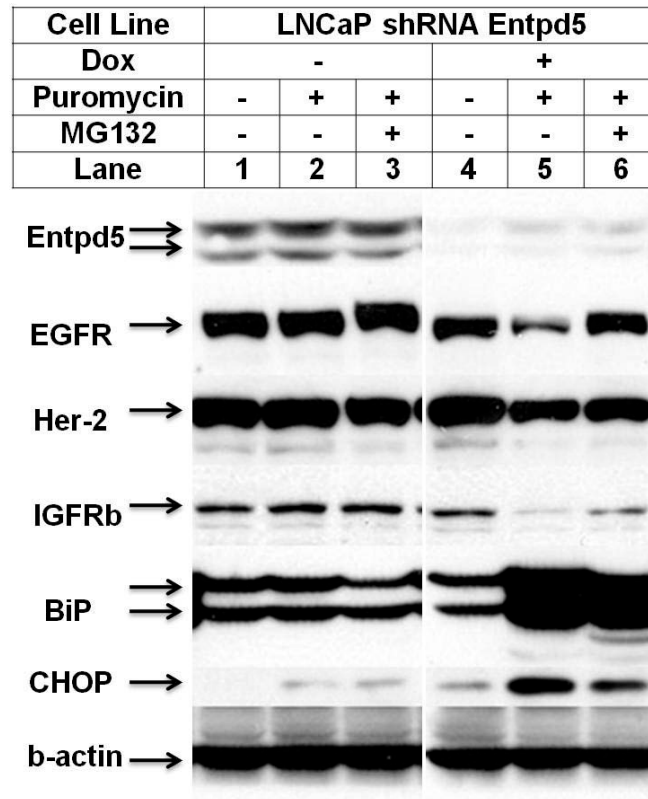


Figure 4-4 Tyrosine Kinase Receptor are degraded in ER-associated degradation pathway

(A) Level of Tyrosine Kinase Receptor (EGFR and HER-2 etc.) decreased rapidly after inducing protein-overloading by puromycin in Entpd5 knocking-down cells.

(B) mRNA expression level of receptor kinase receptors after knocking down Entpd5. mRNA from each cell line was extracted and cDNA was synthesized. EGFR2, Her-2, IGFR, ENTPD5 and β -Actin were amplified from cDNA. mRNA level of EGFR and IGFR β did not decrease after knocking down Entpd5. mRNA of Her-2 was slightly decreased.

(C) Reduction of tyrosine kinase receptors were blocked by proteasome inhibitor MG132.

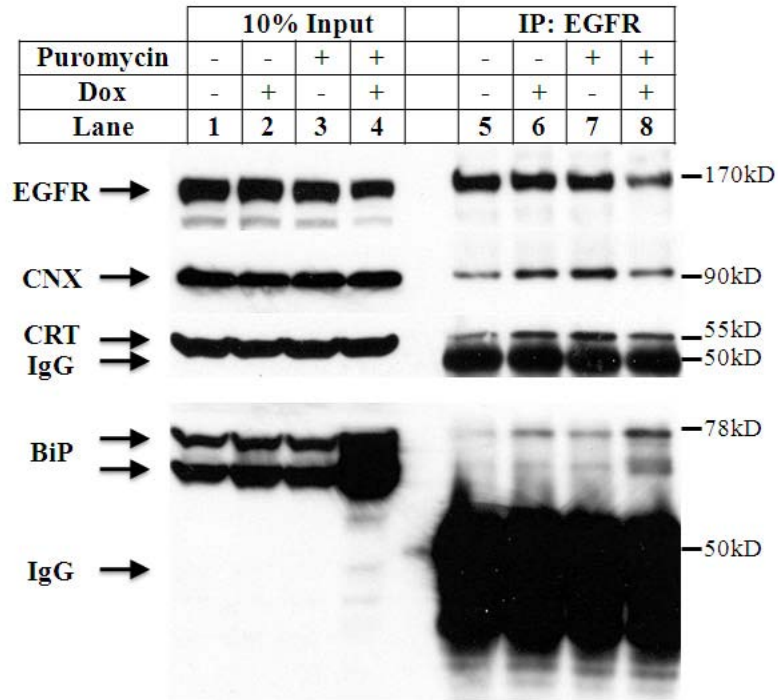


Figure4-5 Co-Immunoprecipitation of EGFR with BiP, CRT and CNX.

Total protein extracts from LNCaP shRNA-Entpd5 cells (without or with dox) were immunoprecipitated with anti-EGFR antibody and analyzed by western blotting with antibody against ENTPD5, BiP, CNX, and CRT.

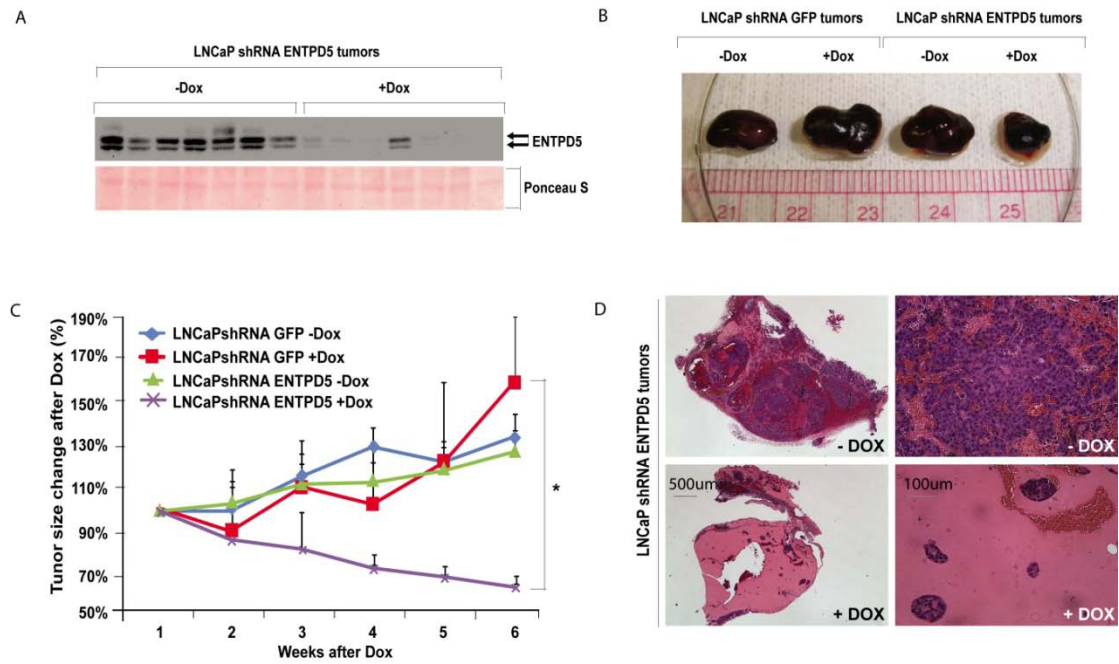


Figure 4-6. Effects of Knocking Down Entpd5 in Xenografts

Tumor growth in nude mice after doxycycline-induced expression of shRNA GFP or shRNA Entpd5. 2×10^6 LNCaP shRNA GFP cells or LNCaP shRNA Entpd5 cells were injected subcutaneously into flank of nude mice. When the tumors reached a volume of approximately around 500 mm^3 , mice were fed with either water with or without doxycycline.

(A) Knockdown efficiency of ENTPD5 in xenograft. Tumors lysates are extracted and aliquots of $20 \mu\text{g}$ of protein were subjected to 10% SDS-PAGE and transfer to nitrocellulose filter. The filter was stained with Ponceau S staining (lower) as loading control followed by western blotting against ENTPD5 (upper).

(B) In vivo knockdown of ENTPD5 shrinks tumor. Representative xenografts from indicated groups are shown.

(C) Time course of tumor shrinkage caused by ENTPD5 knocking down. Tumor size was measured and relative tumor volumes were calculated as described in

Experimental Procedures after mice were fed with or without Doxycycline for indicated time period. Each group consisted of around seven mice. The values are represented as mean \pm SD. * $p < 0.05$.

(D) H&E staining of resected tumors. Left, 2.5X; right, 25X. Upper panel: tumor without Dox. Lower panel: tumor with Dox.

A.

Type	Gene	Species	Localization	Literature description	Reference
I	Entpd5	<i>H.Sapien</i>	ER	N/A	(Trombetta and Helenius, 1999)
	Uda1	<i>C.elegan</i>	N/A	Upregulated in ER stress; no phenotype in loss-of-function	(Uccelletti et al., 2004)
	Gda1	<i>S.cerevisiae</i>	Golgi	Decreased glycosylation of several secreted proteins	(Abeijon et al., 1993)
II	Entpd4	<i>H.Sapien</i>	Golgi	N/A	(Wang and Guidotti, 1998)
	Mig-23	<i>C.elegan</i>	Golgi	Mutant affects glycosylation of ADAM (a disintegrin and metalloprotease) family, MIG-17.	(Nishiwaki et al., 2004)
	Ntp1	<i>C.elegan</i>	N/A	N/A	(Uccelletti et al., 2004)
	Ynd1	<i>S.cerevisiae</i>	Golgi	Decreased glycosylation of several secreted proteins	(Gao et al., 1999)
III	Cant1	<i>H.Sapien</i>	ER	N/A	(Failer et al., 2002)
	Apy1	<i>C.elegan</i>	N/A	Upregulated in ER stress; knockdown induce ER stress	(Uccelletti et al., 2008)

B.

I	Gda1	Uda1	Entpd5
			Entpd6
II	Ynd1	Mig-23	Entpd4
		Ntp1	Entpd7
III	N/A	Apy1	Cant1
Species	<i>S.cerevisiae</i>	<i>C.elegan</i>	<i>H.Sapien</i>

C.

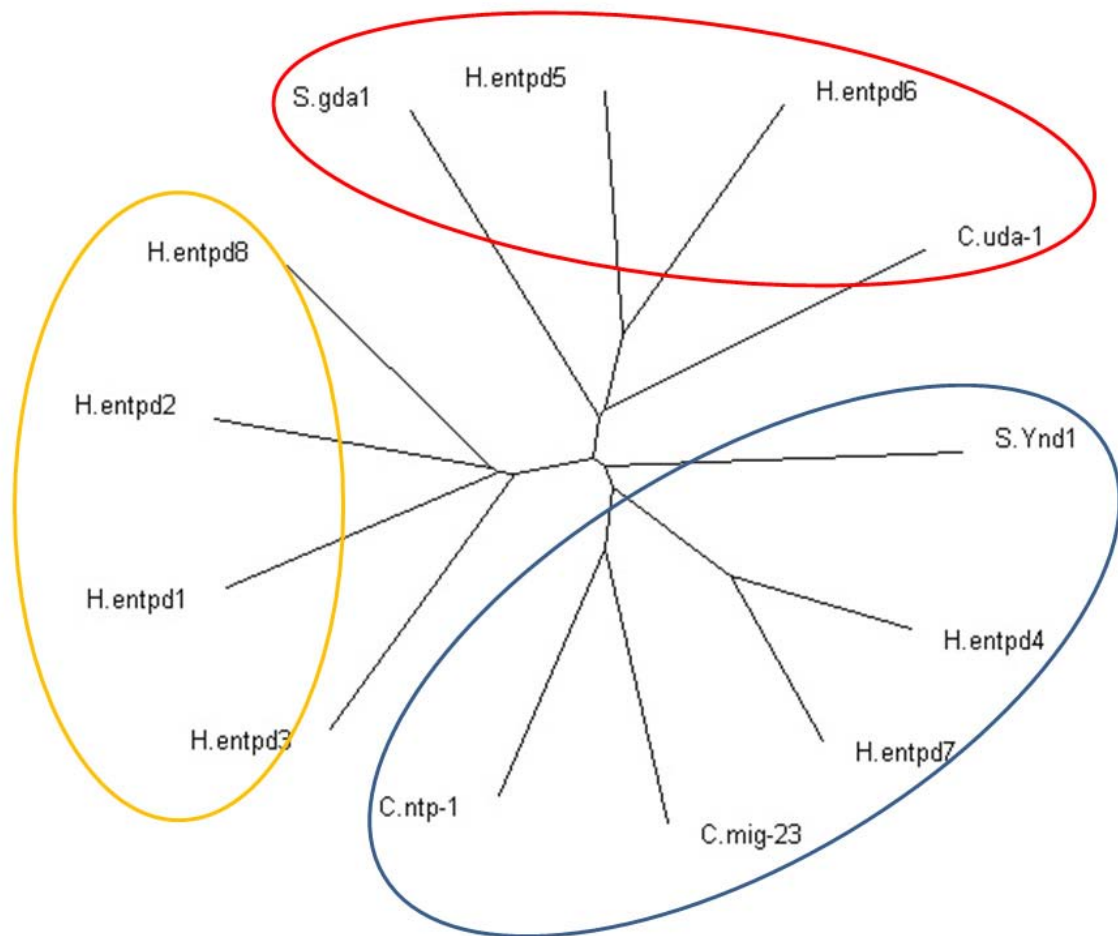


Figure 4-7. Phylogenetic analysis of Entpd family members in different species.

(A).Function and localization of known Entpd5 homologs.

(B).Gene expansion of ER stress-related apyrases from yeast. *S.cerevisiae* has two genes (Gda1 and Ynd1), *C.elegan* has 4 genes (3 of them are homologs of yeast genes and another one Apy1 which does not have homolog in yeast) and *H.Sapien* has 5 genes (4 of them are homologs of yeast genes and another Cant1 which is homolog of Apy1 in *C.elegan*).

(C).Entpd family members can be clustered into 3 different categories according to their sequence similarities. They are conserved from yeast to human.

Reference

Abeijon, C., Yanagisawa, K., Mandon, E., Häusler, A., Moremen, K., Hirschberg, C., and Robbins, P. (1993). Guanosine diphosphatase is required for protein and sphingolipid glycosylation in the Golgi lumen of *Saccharomyces cerevisiae*. *The Journal of Cell Biology* 122, 307-323.

Blobel, G., and Sabatini, D. (1971). Dissociation of Mammalian Polyribosomes into Subunits by Puromycin. *Proceedings of the National Academy of Sciences of the United States of America* 68, 390-394.

Failer, B.U., Braun, N., and Zimmermann, H. (2002). Cloning, expression, and functional characterization of a Ca(2+)-dependent endoplasmic reticulum nucleoside diphosphatase. *J Biol Chem* 277, 36978-36986.

Gao, X.-D., Kaigorodov, V., and Jigami, Y. (1999). YND1, a Homologue of GDA1, Encodes Membrane-bound Apyrase Required for Golgi N- and O-Glycosylation in *Saccharomyces cerevisiae*. *Journal of Biological Chemistry* 274, 21450-21456.

Molinari, M. (2007). N-glycan structure dictates extension of protein folding or onset of disposal. *Nat Chem Biol* 3, 313-320.

Molinari, M., Galli, C., Vanoni, O., Arnold, S.M., and Kaufman, R.J. (2005). Persistent glycoprotein misfolding activates the glucosidase II/UGT1-driven calnexin cycle to delay aggregation and loss of folding competence. *Mol Cell* 20, 503-512.

Nishiwaki, K., Kubota, Y., Chigira, Y., Roy, S.K., Suzuki, M., Schvarzstein, M., Jigami, Y., Hisamoto, N., and Matsumoto, K. (2004). An NDPase links ADAM protease glycosylation with organ morphogenesis in *C. elegans*. *Nat Cell Biol* 6,

31-37.

Oyadomari, S., Yun, C., Fisher, E.A., Kreglinger, N., Kreibich, G., Oyadomari, M., Harding, H.P., Goodman, A.G., Harant, H., Garrison, J.L., *et al.* (2006). Cotranslocational Degradation Protects the Stressed Endoplasmic Reticulum from Protein Overload. *Cell* *126*, 727-739.

Read, R., Hansen, G., Kramer, J., Finch, R., Li, L., and Vogel, P. (2009). Ectonucleoside Triphosphate Diphosphohydrolase Type 5 (Entpd5)-Deficient Mice Develop Progressive Hepatopathy, Hepatocellular Tumors, and Spermatogenic Arrest. *Veterinary Pathology Online* *46*, 491-504.

Ruddock, L.W., and Molinari, M. (2006). N-glycan processing in ER quality control. *J Cell Sci* *119*, 4373-4380.

Trombetta, E.S., and Helenius, A. (1999). Glycoprotein reglucosylation and nucleotide sugar utilization in the secretory pathway: identification of a nucleoside diphosphatase in the endoplasmic reticulum. *EMBO J* *18*, 3282-3292.

Uccelletti, D., O'Callaghan, C., Berninsone, P., Zemtseva, I., Abeijon, C., and Hirschberg, C.B. (2004). ire-1-dependent Transcriptional Up-regulation of a Luminal Uridine Diphosphatase from *Caenorhabditis elegans*. *Journal of Biological Chemistry* *279*:, 27390-27398.

Uccelletti, D., Pascoli, A., Farina, F., Alberti, A., Mancini, P., Hirschberg, C.B., and Palleschi, C. (2008). APY-1, a Novel *Caenorhabditis elegans* Apyrase Involved in Unfolded Protein Response Signalling and Stress Responses. *Mol Biol Cell* *19*, 1337-1345.

Wang, T.-F., and Guidotti, G. (1998). Golgi Localization and Functional Expression of Human Uridine Diphosphatase. *Journal of Biological Chemistry* 273:, 11392-11399.

Summary

PI3 Kinase and PTEN lipid phosphatase control the level of cellular phosphatidylinositol (3,4,5)-trisphosphate, an activator of AKT kinase that promotes cell growth and survival. Mutations activating AKT are commonly observed in human cancers. Activation of AKT and downstream PI3 Kinase signaling activates many downstream targets for cell growth and cell survival, including rapamycin-sensitive mTOR complex 1(mTORC1), which then phosphorylates p70S6K and translation initiation factor 4E-BP1 to accelerate the translational rate, thus promoting rapid cell growth.

Elevated protein translation promotes protein translation, resulting in increased protein flux into ER; this will lead to decreased efficiency of protein folding and accumulation of unfolded proteins in the ER and finally lead to ER stress. How does cancer cell solve this problem of increased folding during rapid growth to avoid ER stress?

We discovered that ENTPD5, an endoplasmic reticulum (ER) enzyme, is up-regulated in cell lines and primary human tumor samples with active AKT. In vitro, ENTPD5 hydrolyzes UDP and generates UMP. ENTPD5 forms a futile cycle with other two enzymes UMPK/CMPK and AK1 to hydrolyze ATP to AMP.

In vivo, ER protein quality control system uses reglucosylation cycle to facilitate protein folding. The reglucosylation cycle generates UDP as a byproduct, which inhibits the key enzyme in reglucosylation step, UDP-glucose:glycoprotein transferase(UGGT). ENTPD5, expressed in ER, hydrolyzes UDP to UMP to relieve inhibition to UGGT,

therefore promoting protein N-glycosylation and folding in ER.

AKT up-regulates ENTPD5 by relieving transcriptional inhibition induced by FoxO transcription factors, accommodating corresponding rapid growth and increased protein influx to ER. Therefore, knockdown of ENTPD5 in PTEN-null cells causes ER stress and thus loss of receptor tyrosine kinases through ER-associated degradation pathway under stress conditions. Consequently, the growth of PTEN-null cells is inhibited both in vitro and in mouse xenograft tumor models for PTEN null prostate cancer cell line LNCaP after knocking ENTPD5.

In conclusion, ENTPD5 is therefore an essential component for PI3K/AKT active cancer cells and a potential drug target for anti-cancer therapy.